Medical image segmentation using MedSAM model

Rendulić, Marijana

Master's thesis / Diplomski rad

2024

Degree Grantor / Ustanova koja je dodijelila akademski / stručni stupanj: **University of Split, Faculty of Science / Sveučilište u Splitu, Prirodoslovno-matematički fakultet**

Permanent link / Trajna poveznica: https://urn.nsk.hr/urn:nbn:hr:166:740621

Rights / Prava: In copyright/Zaštićeno autorskim pravom.

Download date / Datum preuzimanja: **2025-03-14**

zir.nsk.hr

UNIVERSITY OF SPLIT

dabar
DIGITALNI AKADEMSKI ARHIVI I REPOZITORIJI

UNIVERSITY OF SPLIT

FACULTY OF SCIENCE

GRADUATE THESIS

MEDICAL IMAGE SEGMENTATION USING MEDSAM MODEL

Marijana Rendulić

Split, September 2024.

Basic documentation card

MEDICAL IMAGE SEGMENTATION USING MEDSAM MODEL

Marijana Rendulić

ABSTRACT

The use of artificial intelligence is becoming increasingly present in various spheres of modern society, including the field of medicine. This thesis is based on the newest technologies in the field of segmentation (MedSAM) and detection (RCS-YOLO). The algorithms are implemented in a demo application that aims to speed up the process of analyzing large medical image datasets to timely determine a potential suspicious region of the patient's brain, and at the same time to start timely treatment. The paper describes the limitations and further work with the purpose of improving the existing capabilities of the demo application. Also, a detailed methodology related to the dataset, chosen algorithms, and results is given.

Temeljna dokumentacijska kartica

SEGMENTACIJA MEDICINSKIH SLIKA UPOTREBOM MEDSAM MODELA

Marijana Rendulić

SAŽETAK

Upotreba tehnologija umjetne inteligencije postaje sve prisutnija u različitim sferama modernog društva, pa tako i u području medicine. Ovaj rad temelji se na najnovijim tehnologijama u području segmentacije (MedSAM) i detekcije (RCS-YOLO) slike. Navedeni algoritmi implementirani su u demo aplikaciju koja ima za cilj ubrzavanje procesa analize velikih skupova medicinskih slika kako bi se pacijentu pravovremeno otkrila potencijalna sumnjiva regija na području mozga, a samim time i kako bi se pravovremeno krenulo sa tretmanom liječenja. U radu su opisana ograničenja i daljnji rad sa svrhom unapređenja i poopćenja postojećih mogućnosti demo aplikacije. Dana je i detaljna metodologija vezana uz skup podataka, odabrane algoritme i rezultate.

DECLARATION

With which I declare with full material and moral responsibility that I wrote the graduate thesis titled MEDICAL IMAGE SEGMENTATION USING MEDSAM MODEL independently under the supervision of associate professor Saša Mladenović, Ph.D. In thesis, I applied the methodology of scientific research work and used the literature listed at the end of the thesis. Other people's knowledge, attitudes, conclusions, theories, and legalities that I stated directly or paraphrased in the thesis were quoted in the usual, standard way and linked with footnotes to the bibliographic units used. The paper is written in the spirit of the English language.

Student

Marijana Rendulić

Content

Introduction

In medical diagnostics, the accuracy and efficiency of medical image interpretation are crucial for timely and effective treatment. In medicine, magnetic resonance imaging (MRI) is often used, and it represents a technique that offers a detailed insight into the internal structures of the body. There are three types of analysis that depend on the intervention of the expert, and can be divided into manual, semi-automatic and automatic methods. Manual analysis can be time-consuming and prone to human error, given the lack of experts and large amount of MRI data. This can result in a delay in diagnosis and timely treatment. Therefore, the development of efficient, automated techniques is of crucial importance because the use of these algorithms can contribute to the automation of the process of detecting suspicious areas, which can lead to the acceleration of the entire process.

The thesis explores methods whose combination can lead to faster segmentation of suspicious regions on MRI images of brain tumors. The use of machine learning models and application development can improve the diagnostic process, reduce data processing time and increase the accuracy of the abnormality identification. The thesis combines two models, RCS-YOLO and MedSAM, which are integrated into a demo application. The demo application can serve as a starting point in building a comprehensive application for automated analysis and for solving the above-mentioned problems.

1. About research

The purpose of the thesis is to find an appropriate model for the segmentation of medical images, to automate the process of analyzing medical images, especially those related to brain tumors. The acceleration of this process could result in timely diagnosis and timely initiation of treatment. The goal of the thesis is to find and implement models in a demo application that could be further improved. Also, the development of an application that would use selected models would provide comprehensive assistance to the experts in the field of medicine.

This research belongs to the field of technical sciences, field of computer science, and branch of artificial intelligence. According to the type, this is applied research, and according to the methodological approach, the research belongs to quantitative research because the model determines whether the area belongs to the tumor region or not. According to the type of data, the research belongs to the empirical category, because the research is based on the analysis of real data.

1.1. Motivation

In real world, there is often a problem of overloading the health care system. This is contributed by the lack of doctors and the increasing amount of medical data that needs to be analyzed to establish a diagnosis. Therefore, patients often do not receive a timely diagnosis and start treatment. Also, not all doctors have the same level of knowledge. This problem is trying to be solved using artificial intelligence, i.e. machine learning methods. Many researchers work on the problem of automating the process of medical image analysis, with the aim of creating a quality tool that would serve to the experts in the medical field. Thus, the motivation for writing the thesis is to improve the diagnostic process by increasing the precision of labeling structures and reducing the time required for the analysis of large datasets. This would make the process more objective, and the process would be automated, which would lead to a reduction in workload and waiting lists.

1.2. Research questions

This research is focused on automating the process of medical image analysis using machine learning models. More specifically, the goal is to find a segmentation model that will distinguish the suspicious region on the brain image, i.e. healthy and unhealthy brain tissue, with special emphasis on the following research questions:

- Are there models for medical image segmentation? Do they need to be improved?
- Can a suspicious region in brain images be approximated using machine learning models?
- Can the selected models be implemented in an application that would accelerate the process of medical image analysis?
- Are there ethical problems related to the automation of the medical image analysis process?
- Can the whole process be generalized for other organs/tissues?

2. Literature review

Literature review was conducted using the Preferred Reporting Items for Systematic Reviews and Meta-Analyses (PRISMA). [1] The Web of Science (WOS) database was used for the literature review which included reviewed articles from the last two years related to MRI-based brain tumor segmentation. The inclusion criteria were as follows:

- Papers related to brain tumor segmentation in Magnetic resonance imaging (MRI)

- Papers written in English

- Reviewed papers

- Papers published in the last two years (2023., 2024.)

- Publicly available papers

The following exclusion criteria were used to select papers that are not of interest to the thesis:

- Non-reviewed papers

- Papers not written in English

- Papers that are published outside the 2023. and 2024.

- Papers related to other areas such as classification or detection

- Papers that do not use MRI

- Papers in which another area or organ is segmented

- Papers that describe other diseases other than tumors

- Papers that are not publicly available

By applying the mentioned inclusion and exclusion criteria, a total of 23 articles were selected, as can be seen in Figure 2.1.
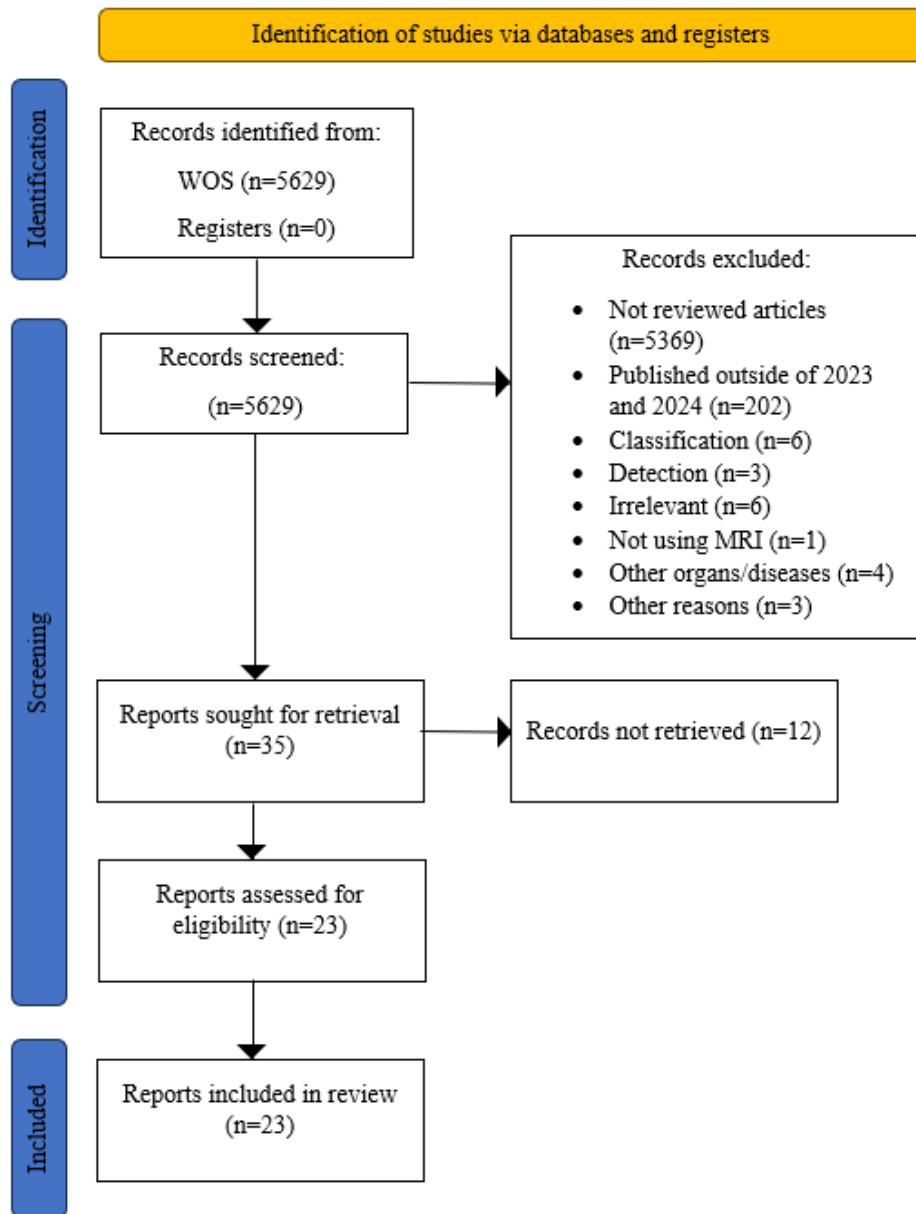
Figure 2.1. PRISMA flow diagram - literature review

2.1. Brain tumor segmentation

Brain tumor segmentation is the differentiation of abnormal brain tissue from healthy brain tissue, and it can be divided into 2D and 3D approaches. [2] Due to limited resources, this thesis focuses on 2D segmentation, where each slice of the brain tumor image is analyzed independently.

Verma A. et al. proposed "Comprehensive Review on MRI-Based Brain Tumor Segmentation: A Comparative Study from 2017 Onwards" [2], which reviews automated brain disease diagnosis and tumor segmentation methods from 2017 to 2024. According to

[3] in the earlier days brain tumor segmentation methods were divided depending on the need for manual intervention into manual, semi-automated, and fully automated methods. Verma A. et al. [2] categorize the methods into three classes, i.e., conventional methods, machine learning-based methods, and deep learning-based methods which can further be divided into subcategories as shown in Figure 2.1.1.
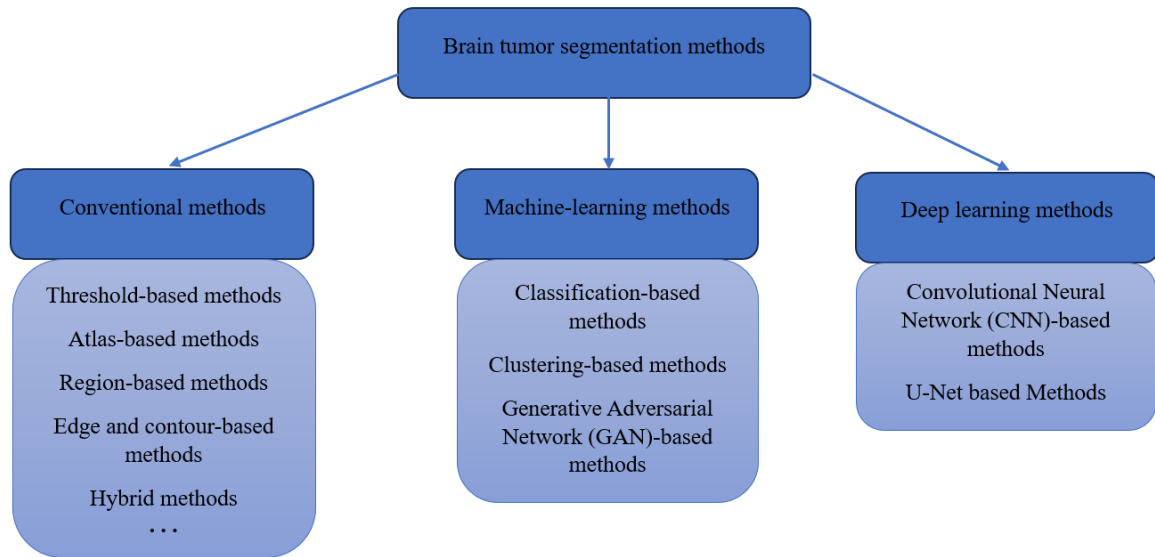
Figure 2.1.1. Brain tumor segmentation methods

2.1.1. Conventional methods

Conventional methods can be divided into categories, i.e. threshold-based, atlas-based, region-based, etc. as shown in Figure 2.1.1., and some of them will be further explained bellow.

The threshold-based methods [70] apply one or more thresholds to the grayscale intensity values of different MRI modalities, such as T1-weighted, T2-weighted, contrast-enhanced T1-weighted (T1C), and Fluid Attenuated Inversion Recovery (FLAIR). [2] Grayscale intensity values are used as features to divide the image into several segments based on the applied threshold which reduces processing time by avoiding additional feature extraction, but it does not perform accurately for brain tumor segmentation. This approach is useful for highlighting enhanced tumors in T1C MRI and identifying tumor boundaries in T2 images. [2]

Atlas-based methods use a map of a healthy brain's anatomy, including gray matter (GM), white matter (WM), and cerebrospinal fluid (CSF). These approaches help in gaining prior

knowledge of the modality by co-registering the atlas with the input image, followed by segmentation of various subcomponents or regions. [2]

Region-based methods segment an image into multiple disjoint regions based on predefined similarity measures, that rely on specific pixel features, which are then combined to form image regions. In this method, a seed point is selected and, based on the pixel feature is then compared with all other pixels to partition them into two regions – one similar to the seed pixel and the other dissimilar. [2]

However, each method has its challenges. For example, threshold-based methods can have a problem of misclassifying brain tumor tissues because different tissues can have similar intensity values. Region-based methods suffer from under-segmentation or over-segmentation because those methods might struggle with the heterogeneity of brain tumors. Edge and contour-based methods may encounter a problem in the adherence of insufficiently well-defined tumor boundaries. Contour-based methods [71] rely on an initial contour, which can be set manually or automatically, that diverges or converges around the object of interest. [2]

Conventional methods are appreciated for their simplicity and lack of dependence on prior knowledge, but they often don't provide the accuracy required for reliable disease diagnosis. [2] Therefore, the focus is on more complex methods with better performance that follow in the rest of the thesis.

2.1.2. Machine-learning methods

Machine learning methods can be divided into classification-based and clustering-based methods, as well as generative adversarial networks (GANs) as shown in Figure 2.1.1.

Classification and clustering are key branches of machine-learning methods that recognize patterns from which conclusions are drawn depending on the provided data. Generative Adversarial Networks (GANs) should also be mentioned here, which in an unsupervised way generate data using random noise. [2] Each of them is explained below.

Numerous machine learning (ML) methods with a discriminating approach have been proposed for the automatic segmentation of medical images, such as Neural Networks, Support Vector Machine (SVM), Random Forest (RF), fuzzy clustering, etc. Those methods don't require anatomical brain information for model development which is opposite to the generative methods that segment abnormal brain regions regarding the anatomical structure

of healthy and tumorous tissues. [2] Several studies applied RF classifier to segment brain tumors over different features, such as statistical, wavelet, texture-based, context-sensitive, local, and contextual patch-based features. [4-8] Support Vector Machine (SVM) is a popular supervised machine learning algorithm that finds a maximum margin hyperplane to classify data points in two or more dimensions. [2] SVG has been exploited by researchers for detecting and segmenting abnormal tumors using different features (statistical, texture) and different kernels (Sigmoid, linear, Radial Basis Function). [9-11] Artificial Neural Network (ANN) is also a commonly used machine learning algorithm for image classification, although the performance of the ANN depends on several parameters like model complexity (i.e., the number of hidden layers), activation functions, number of features, and feature extraction. [2] Researchers have used different variations of ANNs [12], including Deep Belief Network (DBN) [14, 15] and autoencoders [13] which represent high-dimensional data in a lower-dimensional space. [2] However, a significant limitation of classification models is the quality and efficiency of extracted features. Recent research introduces more advanced techniques such as the use of deep neural networks. Yet, with deep learning, concerns arise about the benefits of adding layers due to degradation, where increasing depth initially improves accuracy but also leads to rapid decline. [2]

The above-mentioned supervised classification algorithms are popular for brain tumor segmentation due to their high performance and the availability of large, annotated datasets. However, unsupervised algorithms are used for unannotated real datasets. [2] Researchers used different unsupervised algorithms for brain abnormalities detection and segmentation, like Fuzzy C-means (FCM) [16, 17], Self-Organizing Map (SOM) [18], Active Contour Model (ACM) [18], etc., as well as various nature-inspired optimization algorithms with unsupervised clustering methods to enhance the performance of tumor detection. [2] Moreover, K-means clustering is often used in combination with other algorithms such as OTSU [19] or CLAHE [20]. Although unsupervised learning approaches have advantages, the issue is that the found patterns may not correspond to the actual segmentation of the tumor, especially in noisy images or MRI images with artifacts. [2]

Generative Adversarial Networks (GANs) are unsupervised algorithms consisting of a generator and a discriminator. The generator generates data based on random noise, and the discriminator classifies data as real or fake. Real data is considered training data, and generated data is considered as fake one. Furthermore, the discriminator's feedback helps the generator and discriminator improve iteratively. [2] Several studies [21-27] have used

GANs for brain tumor detection, classification, and segmentation, although they can be challenging to train due to issues like mode collapse, and the generated images may require validation against clinical standards. [2] GANs can be used across different datasets and modalities, but their performance may vary. That suggest that machine-learning approaches may need tuning and validation for specific applications, which may limit their ability to generalize effectively. Also, there is a challenge of lack of interpretability regarding generating and selecting features, which can be a barrier to clinical adoption. [2]

Considering the complexity of the model and the large amount of data, the applicability of these algorithms in real-time, as well as in applications in a clinical environment, is questionable. According to [2], SVM is the most preferred machine-learning technique, and the performance of machine-learning approaches stagnates as the dataset increases.

2.1.3. Deep learning methods

Machine learning methods rely on medical expertise to extract meaningful features for model training, which often results in low accuracy, especially when distinguishing between unclear boundaries of healthy and lesion tissues. In contrast to handcrafted feature extraction, convolutional deep-learning methods automatically extract a wide range of features using convolution and pooling operations, followed by a fully connected layer (Figure 2.1.3.1), leading to improved accuracy, especially with growing datasets. [2]
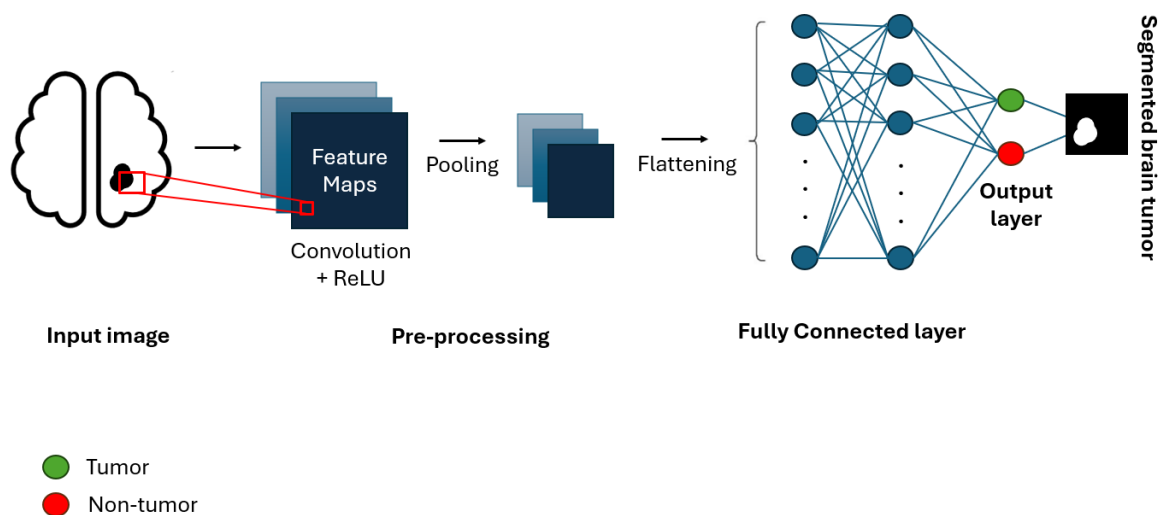

Figure 2.1.3.1. Convolutional neural network (CNN) for brain tumor segmentation [2, 51]

CNNs have been used in image classification tasks. However, U-Net is used for brain tumor segmentation, often outperforming CNNs due to their unique encoder-decoder U-shaped architecture that preserves spatial information through skip connections and excels in medical image analysis. [2] Both CNNs and U-Net will be further explained below.

Wang et al. [28] used 12-layer CNN for brain tumor segmentation, which improved accuracy compared to traditional segmentation methods. Zhoa et al. [29] proposed a model combining fully connected neural networks (FCNNs) with conditional random fields (CFRs) to enhance accuracy and preserve spatial information. [2] Other studies proposed various CNN architectures, like 3D CNNs [30], cascaded networks [31], or deep convolutional networks [32]. [2] Iqbal et al. [33] presented innovative architectures, SkipNet, IntNet, and SENet, that demonstrated innovations like replacing innermost network blocks with skip connections or integrating SE block. [2] Naceur et al. [34] proposed three deep CNN models, 2CNet, 3CNet, and EnsembleNet. In those models, the number of blocks differs, and EnsembleNet executes and fuses the results of both 2CNet and 3CNet models. [2] Kamnitsas et al. [35] used residual networks in a 3D CCN model to minimize the vanishing gradient descent problem, by increasing the number of layers in deep neural networks. [2] For automatization of brain tumor segmentation, Pereira et al. [36] used a hierarchical approach, and Mittal et al. [37] used stationary wavelet transform (SWT) for feature extraction, and growing CNN for lesion classification. [2] Togocar et al. [38] used CNN model that incorporated an attention module (emphasizing the relevant regions of MR images which saved processing time), a residual network, and the hypercolumn technique. [2] Huang et al. [39] proposed an architecture based on adaptive gamma correction (AGC) that focuses on regions with valuable information, and consequently enhance local features and improve performance. [2] Rafi et al. [40] introduced a 3D multi-level CNN model that used dilated convolutions with different kernel sizes for glioma segmentation. [2] Hu et al. [41] fused multi-cascaded CNN with fully connected conditional random fields (CRFs) to preserve local information, and Ranjbarzadeh et al. [42] addressed overfitting with cascaded CNN that processes small image patches, which reduces computational time and improves local feature enhancement. [2] Deng et al. [43] utilized heterogeneous CNN (trained with MRI patches) and CRFs (trained on image slices), while Khan et al. [44] used handcrafted features to train deep learning CNN model. Features from MRI were extracted using local binary patterns (LBP), histogram of oriented gradients (HOG), and mean intensity. [2] Myronenko and Hatamizadeh [45] introduced a symmetrical encoder-decoder CNN, and Aswani and

Menaka [46] CNN-based model used both vertical and horizontal patches during training. [2] Huang et al. [47] proposed an architecture to fuse up-sampled multi-scale features, that were extracted using convolutional and maxpooling operations. [2] Aggarwal et al. [48] solved deep-learning gradient problems using a residual network (ResNet), thus improving the precision and learning speed. [2] Other significant contributions included a 3D multi-scale ghost CNN with an auxiliary MetaFormer decoding path [49], and an active learning approach with NiftyNet to train CNN [50]. [2] The development of CNN-based techniques enhanced accuracy, sensitivity, and specificity. Despite that, key challenges like generalizability, interpretability, computational efficiency, etc. still persist. [2] Some of those challenges will be addressed later in the thesis.

Successful training on deep neural networks demands a large number of annotated data. Ronneberger et al. [52] proposed a network architecture and training strategy that utilizes available annotated data through data augmentation such as shifts, rotations, and deformations – common issues in medical images. The architecture, known as U-Net, consists of a contracting path and an expansive path, which can be seen in Figure 2.1.3.2. The contracting path captures context, and the expansive path allows precise localization. [52] In the contracting path, also known as the encoder, a sequence of convolution and maxpooling operations are performed to reduce input image dimensions. In an expensive path, i.e. decoder, images are up-sampled using deconvolution operations to identify tumor cell locations. Convolution and deconvolution blocks are connected through skip connection to preserve spatial information. [2] This architecture enables end-to-end training from a relatively small number of images. [52] Also, a key innovation in U-Net is the ability to handle large images using an overlap-tile strategy, where the network predicts border pixels by extrapolating context from mirrored input images which makes U-Net useful for biomedical tasks. [52] According to [2], deep-learning-based methods, particularly different variants of the U-Net model, achieve better results than other approaches for brain tumor segmentation. Many researchers provided various modifications of the U-Net model, and some of them will be explained below.
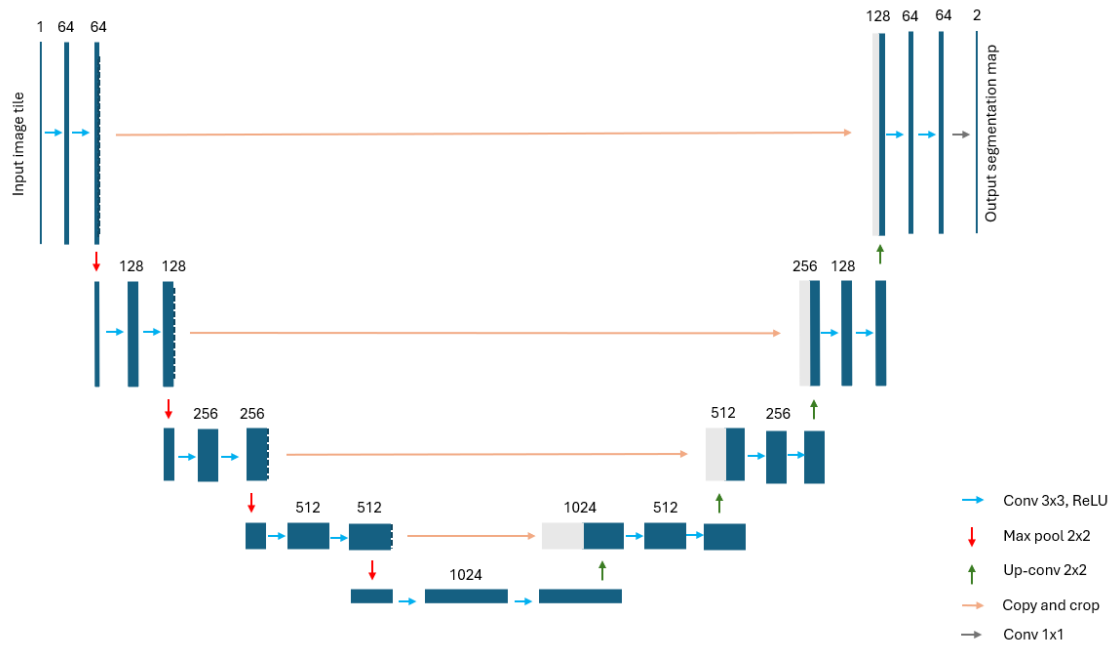
Figure 2.1.3.2. U-Net architecture [52]

Ding et al. [24] introduced a two-stage brain tumor segmentation model, where the first stage used U-Net for coarse segmentation, preserving local spatial information, while the second stage used a convolution-based encoder-decoder model that refined the segmentation. [2] Zhu et al. [53] introduce Large deep 3D ConvNets with automated Model Parallelism (LAMP) while investigating the impact of model and input size on segmentation accuracy. They validated different U-Net models (3D U-Net, 3D Squeeze-and-Excitation U-Net) in segmentation tasks, and designed a parallel U-Net-based GPipe as the back-end parallelism. The authors concluded that employing large models and input context increases segmentation accuracy, and large inputs reduce inference time by leveraging automated model parallelism. [53] LAMP design can be seen in Figure 2.1.3.3., which illustrates the minimization of dependency on skip connections in U-Net by splitting it into two separate blocks. This design enables U-Net to achieve more parallel blocks, which results in higher throughput. [53]

12

Figure 2.1.3.3. LAMP: reduction of skip-connection dependency (a)) by separating it into two blocks (b)) [53]

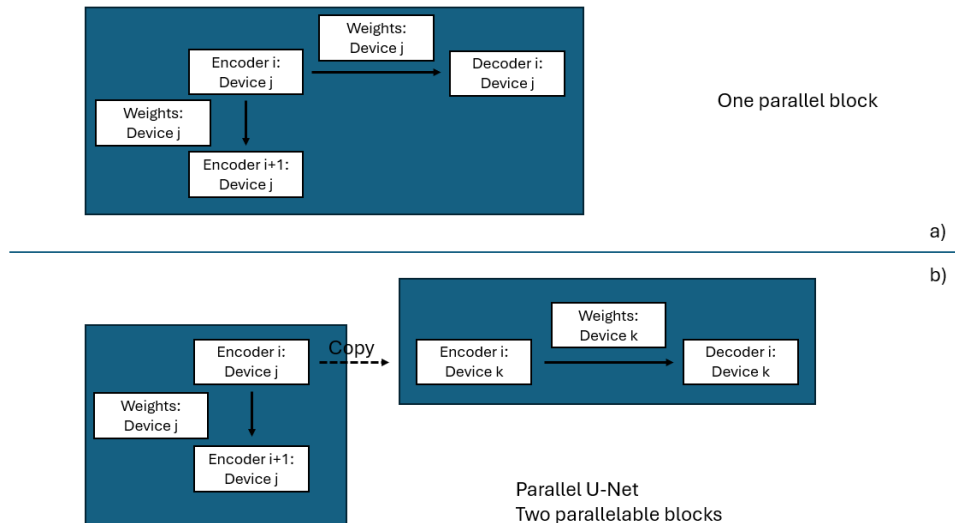Lie et al. [54] proposed a new V-net-based deep learning model with encoder-decoder architecture, with batch normalization and replacement of original residual blocks with bottom residual blocks. This model was introduced to improve the accuracy of the existing V-net CNN model. [2] Naser and Deen [55] proposed a hybrid model with U-Net [52] for segmentation, VGG16 for grading, and a fully connected network at the end. [2] Zhang et al. [56] combined residual models and attention gates in the U-Net framework, enhancing silent features and suppressing irrelevant information, thus improving segmentation accuracy. [2] Lin et al. [57] addressed the problem of information loss in U-Net during up-sampling and down-sampling by placing convolution operations and designing a model to strengthen voxel relationships, thus preserving spatial information. [2] Ma et al. [58] modified the Attention U-Net model to introduce MRDS and APR models by incorporating deep supervision and residual blocks. These modifications extracted rich features, captured boundary information, and addressed issues like overfitting and vanishing gradient descent problems. [2] Some of the authors replaced the encoder path with other architectures like ResNet50 [59] or MobileNetV2 [60]. Also, a lightweight 3D U-Net model was invented by Xiao et al. [61] when each encoder-decoder layer was modified to have 32 channels. [2] Zhou et al. [62] introduced a U-Net-based multi-encoder network for brain tumor segmentation to address the challenge of missing modalities by generating an artificial missing modality with enhanced features. [2] Several researchers used residual blocks in the encoder or decoder path, or both [63-67]. Ruba et al. [68] combined U-Net with ResNet and integrated skip connections with attention gates to improve brain tumor segmentation

13

accuracy which enhanced tumor localization and overall tumor segmentation. [2] Yu et al. [69] presented an U-Net-based model to handle volumetric data, which was subdivided into hierarchical patches and segmented into blocks. Blocks were processed by a transformer encoder, followed by pooling and skip connections featuring residual blocks. [2]

Many researchers customized the U-Net model by adjusting its depth and width for segmentation optimization. Adding residual connections into the U-Net structure minimized the vanishing gradient problem, and adding attention gates into skip connections filters unnecessary information passed between the encoder and decoder. Despite these improvements, U-Net models still face challenges like overfitting to limited labeled data, or computational costs. Further improvements may include developing hybrid models that combine other architectures with U-Net. [2]

Deep learning models have many advantages, but they require extensive computational resources and large annotated datasets. Also, they can operate as "black boxes" that do not give insights into decision-making processes, which can be a problem when it comes to interpretability in clinical applications. Overfitting also remains a challenge, so the use of sophisticated regularization techniques and careful model validation are mandatory. [2]

2.2. The dataset

The BRATS-2013 [72] dataset includes 3D MRI volumes from 20 high-grade (HG) gliomas and 10 low-grade (LG) glioma patients, with each subject data having four MRI images: T1C, FLAIR (Fluid-attenuated inversion recovery), T1-weighted, and T2-weighted images. These volumes consist of 176 slices of 2-dimensional images, each 216x176 pixels. The BRATS-2015 dataset [73] expands this to 220 HG and 54 LG glioma subjects, with 155 slices per volume, each 240x240 pixels. In both datasets, the skull is removed to protect the subjects' identities. Subsequent versions of BRATS (2017-2021) retain the core characteristics of the BRATS 2015. [2]

The Cancer Imaging Archive (TCIA) [74] is another publicly available brain tumor detection and segmentation dataset that covers a wide range of cancer types. BrainWeb [75] is a synthetic dataset that contains simulated brain MRI images with T1, T2, and proton density (PD) modalities. [2] According to [2], despite those two datasets, as well as other options [78, 79, 87-91], the BRATS dataset remains the most popular for brain tumor segmentation.

3. Technical overview

The technical overview contains the main methods, datasets, and metrics used further in the thesis. The following sections review RCS-YOLO [76] used for brain tumor detection, giving technical aspects related to the network architecture. Furthermore, the section provides information about MedSAM [77] used for brain tumor segmentation, as well as Br35H [78] and LGG [79] datasets used for model training and evaluation, i.e. concluding the application development process.

3.1. Brain tumor detection

Brain tumor detection is the task of identifying suspicious regions, i.e. tumors within a brain image. In the context of AI, many detection techniques were proposed to analyze imaging data with high accuracy, thus assisting in the early detection of brain tumors. In the thesis, the detections were needed to serve as an input to the segmentation model to specify the segmentation target. In the following subsection, more details are given about the RCS-YOLO algorithm, its performance, and its architecture.

3.1.1. RCS-YOLO

YOLO frameworks are one of the most efficient object detection algorithms, but their effectiveness in brain tumor detection has not yet been sufficiently investigated. Kang et al. [76] proposed a YOLO-based model for brain tumor detection, which was trained on the Br35H dataset, and outperformed the YOLOv6, YOLOv7, and YOLOv8 in speed and accuracy. The accuracy of RCS-YOLO exceeds that of YOLOv7 by 1%, and the inference speed by 60% at 114.8 frames per second (FPS).

RCS-YOLO architecture consists of RCS-OSA and RepVGG modules as shown in Figure 3.1.1.1. The number of stacked RCS modules is represented with n, and n_{cls} represents the number of classes in detected objects. Detection layers obtained using 2D convolutional networks are labeled with IDetect. [76]

RepVGG/RepConv ShuffleNet is an architecture designed as a structural reparametrized convolution based on channel shuffle. Input tensor splits into two equal parts, where one part undergoing a process involving the identity branch, 1x1 convolution, and 3x3

convolution to construct the RCS, and RepConv comes from the transformation of the identity branch, 1x1 convolution, and 3x3 convolution during inference stage with the help of structural reparameterization. A channel mixing operator is used, which reduces computational complexity. Also, channel mixing enables efficient communication of information between features, which allows a more informative feature representation. So, this reduces the computational complexity and inference-time memory consumption, resulting in faster inference. [76]

RCS-OSA module is developed by incorporating RCS, that was mentioned in paragraph above. At different locations of the network, different numbers of stacked RCS modules are used, thus ensuring reuse of features and improving the flow of information between different channels, i.e. between features of adjacent layers. [76]

Figure 3.1.1.1. RCS-YOLO architecture [76]

RCS-OSA + Upsampling and RCS-OSA + RepVGG/RepConv Undersampling perform alignment of feature maps of different sizes and thus enable the exchange of information between the two prediction feature layers, which enables fast inference of high accuracy in object detection. Moreover, RCS-OSA reduces the memory access cost (MAC) by maintaining the same number of input channels and minimum output channels. [76]

For network building, authors used max-pooling undersampling 32 times of YOLOv7 for backbone network construction and RepVGG/RepConv with a step of 2 for undersampling. To further reduce the inference time, the authors reduce the number of detection heads from 3 to 2, which also reduces the number of convolutional layers and the computational complexity of RCS-YOLO. Also, this reduces the total computational requirements of the network and the computational time required for the postprocessing non-maximum suppression. [76]

3.2. Brain tumor segmentation

Segmentation is often used in medical image analysis to identify the region of interest (ROI) such as organs, lesions, and tissues. Manual segmentation is a time-consuming process, and this problem can be solved by using fully or semi-automated segmentation. Earlier mentioned deep-learning models often have task-specific nature and their performance can be significantly worse when applied to new tasks or different data types. [77] In the next subchapter, the Segment Anything in Medical Image model (MedSAM) is proposed, which with its architecture contributes to solving the generalizability problem.

3.2.1. MedSAM

MedSAM [77] model is developed for medical image segmentation, thus solving the problem of lack of generalizability of other models. The model was developed using an extensive medical image dataset containing 1,570,263 image-mask pairs, spanning 10 different imaging modalities (Figure 3.2.1.1.) and more than 30 types of cancer. The dominant modalities in the dataset are magnetic resonance imaging (MRI), computed tomography (CT), and endoscopy, but there are also others such as ultrasound, X-Ray, pathology, fundus, dermoscopy, mammography, and optical coherence tomography (OCT). The diversity of these modalities requires a universal and efficient model for handling the unique characteristics of each modality. [77]

The model was evaluated across 86 internal and 60 external validation tasks, showing better accuracy and robustness compared to models specialized for individual modalities. MedSAM shows efficiency in segmentation across various tasks, thus showing potential to be a part of diagnostic tools and treatment plans. [77]
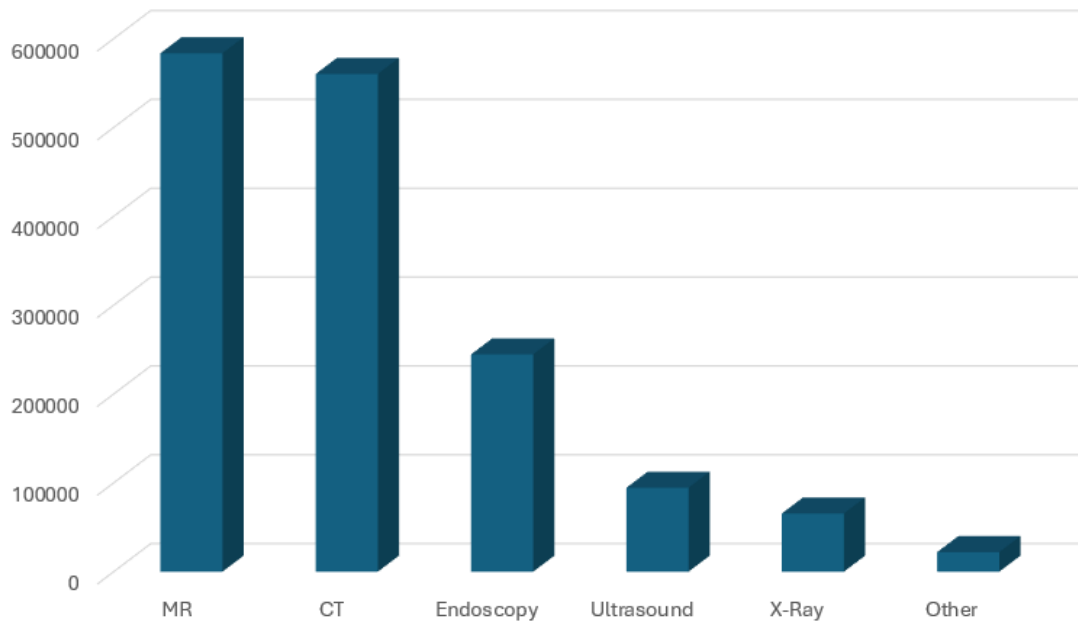
Figure 3.2.1.1. Modality distribution in the dataset [77]

The earlier mentioned diversity of modalities brings concerns about the choice of model architecture, considering that with the same model, it should be possible to segment different modalities and ROIs. Authors of the MedSAM proposed a practical approach and developed a 2D segmentation model, that can adapt to specific tasks based on user-provided prompts. Also, the model processes 3D images as a series of 2D slices, so it can handle both 2D and 3D modalities. When it comes to user prompts, they include points and bounding boxes as can be seen in Figure 3.2.1.2. [77]

The previously mentioned bounding boxes provide spatial context for the ROI, which allows the algorithm to more precisely determine the target area for segmentation. The effectiveness of bounding boxes is especially evident in the multiple object segmentation. On the other hand, point-based prompts can be ambiguous, especially with similar structures. [77]
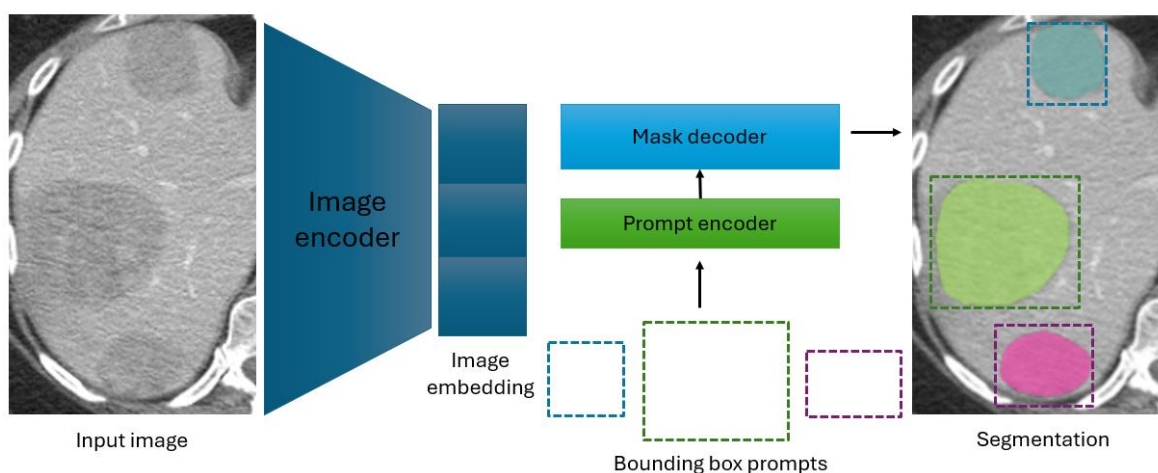
Figure 3.2.1.2. MedSAM Network Architecture [77]

The MedSAM Network Architecture consists of a vision transformer (ViT)-based image encoder that maps the input image into a high-dimensional image embedding space, a prompt encoder that transforms bounding boxes into feature representations using positional encoding, and a mask decoder that fuses the image embedding and prompt features using cross-attention. [77] The architecture is shown in Figure 3.2.1.2.

The authors [77] also conducted a study that used experts for annotations. The experts manually annotated 3D tumors slice-by-slice, as well as drew long and short tumor axes with linear markers every 3-10 slices. MedSAM was then used to segment the tumors based on the linear annotations, and experts revised the segmentations. The results show that MedSAM has reduced annotation time by 82.37% and 82.95% compared to the two experts. [77] These results show the potential of MedSAM in the automation annotation process of segmenting suspicious regions and will be used in the continuation of the thesis.

3.3. The datasets

The chosen datasets used further in the thesis are the Br35H dataset [78] and the LGG Segmentation Dataset [79].

The Br35H dataset consists of 1500 brain MRI images that are tumorous and 1500 images that are non-tumorous. [78] The reason why the Br35H dataset was chosen is that the authors of the RCS-YOLO model [76] claim that the model trained on that dataset gives better results when evaluated on the publicly available brain tumor detection annotated datasets than other state-of-the-art YOLO models.

LGG Segmentation Dataset includes MR images of the brain along with manually created FLAIR abnormality segmentation masks. The images were obtained from The Cancer Imaging Archive (TCIA) and they represent 110 patients who are a part of The Cancer Genome Atlas (TGCA) lower-grade glioma collection. Each patient has at least a fluid-attenuated inversion recovery (FLAIR) sequence and associated genomic cluster data. [79] The reason why the LGG Segmentation Dataset was used in the experiment is the fact that the MedSAM model [77] was trained on the extensive dataset mentioned above, which was obtained from various sources, including the TCIA archive, Kaggle, Grand-Challenge, Scientific Data, CodaLab, and various other segmentation challenges. Considering mentioned, there is a possibility that this dataset was not used in model training since it was not explicitly specified as the training data. However, there is a possibility that it was used because the images were obtained from the TCIA, which can be a potential limitation due to using it for test purposes.

The Br35H dataset was used for the first part of the experiment, and the LGG Segmentation Dataset was used in both the first and second parts of the experiment. The details of the experiment are explained in Chapter 4 of the thesis.

4. The experiment

The main idea of the thesis is a faster analysis of large datasets of medical images, specifically targeting suspicious areas that may indicate a brain tumor. To do that, detection and segmentation methods are used. The experiment is conducted in two parts: the first part aims to find a way of successful detection and segmentation that are further used in the second part – distinguishing between suspicious and non-suspicious images using the graphical user interface (GUI). The GUI part of the experiment will be explained separately in Chapter 5.

As explained earlier, for successful segmentation using the MedSAM model [77], it is necessary to determine the region of interest (ROI). The ROI determination is based on drawing the bounding boxes sent into the prompt encoder of the MedSAM model, and their drawing is attempted to be automated by using the RCS-YOLO detection model. In the GUI, both automated and manual drawings of the bounding boxes will be covered, but in this chapter, the focus is on finding the best way to make an automatic one.

4.1. RCS-YOLO model training using Br35H dataset

The authors of the RCS-YOLO [76] trained the model on the Br35H dataset. Also, the authors claim that the model, when evaluated on publicly available brain tumor detection annotated datasets, showed better accuracy and speed than other state-of-the-art YOLO models. Considering the mentioned and the fact that pre-trained weights were not accessible, in the thesis, RCS-YOLO was trained on the Br35H dataset, and the obtained model was further used as an input to the MedSAM model. First, we will propose the process of training the RCS-YOLO model.

The model was trained following the command line:

```
!python train.py --workers 8 --device 0 --batch-size 32 --
data data/br35h.yaml --img 640 640 --cfg cfg/training/rcs-
yolo.yaml --weights '' --name rcs-yolo --hyp
data/hyp_training.yaml
```

<div align="center">Code 4.1.1. RCS-YOLO model training</div>

The free version of Google Colab was used for the training environment due to the possibility of using the Tesla T4 GPU graphics card. Graphics card details are as follows:

- Driver Version: 535.104.05

- CUDA Version: 12.2

- 16 GB VRAM

The hyperparameters are defined in `hyp_training.yaml`, and there are some differences from the default values [80]. The differences are as follows:

- `lrf: 0.08` : final learning rate used to adjust the learning rate over time [80]

- `box: 0.05` : weight of the box loss component in the loss function, determines the level of importance assigned to accurately predicting bounding box coordinates [80]

- `translate: 0.2` : Horizontal and vertical image translation by a fraction of the image size, helping to learn to detect partially visible objects [80]

- `scale: 0.85` : Scales the images according to the gain factor, simulating the appearance of objects at various distances from the camera [80]

- `flipud: 0.5` : Flips the image upside down concerning the specified probability, increases the data variability [80]

The `inference.py` script is modeled after the `test.py` script, which was adapted for real-time inference purposes. The inference was run using the `best.pt` model on the LGG dataset to determine the bounding boxes that are further used as input to the prompt encoder of the MedSAM model. Examples are shown in Figure 4.1.1. where predicted bounding boxes obtained from RCS-YOLO are represented in the first column, the ground truth segmentation mask in the second column, and the predicted segmentation mask obtained from MedSAM in the third column. Three examples are shown as follows:

a) Shows quite accurate bounding box prediction, as well as a segmentation mask close to the ground truth segmentation mask.

b) Shows the bounding box and segmentation mask prediction of a non-existing tumor.

c) Shows an incorrect bounding box prediction, and thus segmentation mask prediction. The ground truth segmentation mask is much smaller than the predicted one, and it is located in the bottom right part of the brain.
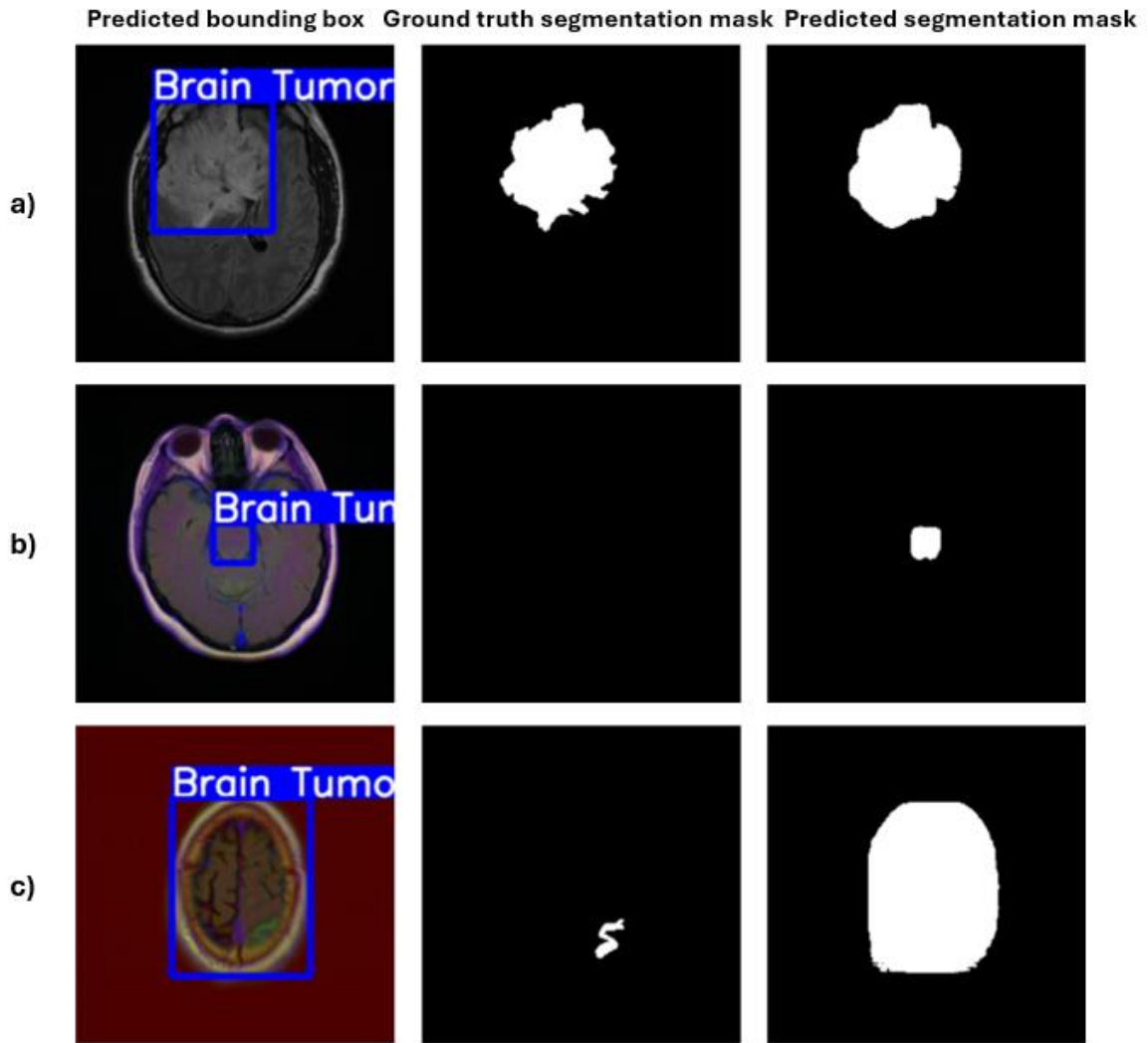
Figure 4.1.1. Examples of RCS-YOLO and MedSAM model predictions

Given that MedSAM model predictions directly depend on RCS-YOLO predictions, the next step is to work on the potential improvements of the RCS-YOLO detections. The idea is to train the model on the ground truth bounding boxes of the LGG Segmentation Dataset. Considering that the LGG Segmentation Dataset does not contain ground truth bounding boxes of the tumors, pseudoannotations obtained using segmentation masks will be used. More about this approach will be explained in the following chapter.

4.2. RCS-YOLO model training using pseudoannotations

The second approach aims to improve the RCS-YOLO detections, making the predicted segmentation masks more precise. To do that, pseudoannotations of bounding boxes were determined using the segmentation masks of the LGG Segmentation dataset. The LGG

Segmentation Dataset was separated into train (60%), valid (20%), and test (20%) sets. The following function was used to extract the bounding box from the segmentation mask:

```python
def mask_to_bbox(mask):
    contours, _ = cv2.findContours(mask, cv2.RETR_EXTERNAL,
cv2.CHAIN_APPROX_SIMPLE)
    if len(contours) == 0:
        return None
    x, y, w, h = cv2.boundingRect(contours[0])
    return x, y, w, h
```

Code 4.2.1. Extraction of bounding box from segmentation mask

Furthermore, the structured annotation dictionary was made and later used for model training and evaluation. The Code 4.2.2. checks the corresponding mask file for each image, extracts the bounding box of the object using the mask, and stores this information as a rectangle in the annotation:

```python
for image_file in image_files:
    filename = os.path.basename(image_file)
    size = os.path.getsize(image_file)

    mask_file = os.path.join(mask_dir,
filename.replace('.tif', '_mask.tif'))
    if os.path.exists(mask_file):
        mask = cv2.imread(mask_file, cv2.IMREAD_GRAYSCALE)
        bbox = mask_to_bbox(mask)
        if bbox:
            x, y, w, h = bbox
            regions = [{
                "shape_attributes": {
                    "name": "rect",
                    "x": x,
                    "y": y,
                    "width": w,
                    "height": h,
                },
                "region_attributes": {}
            }]
            # Create annotation entry
            annotations[filename + str(size)] = {
                "filename": filename,
                "size": size,
```

```
            "regions": regions,
            "file_attributes": {}
        }
```

Code 4.2.2. Extraction of bounding box from segmentation mask

The extracted bounding box represents the smallest rectangle that can enclose the region of the mask, as shown in Figure 4.2.1.
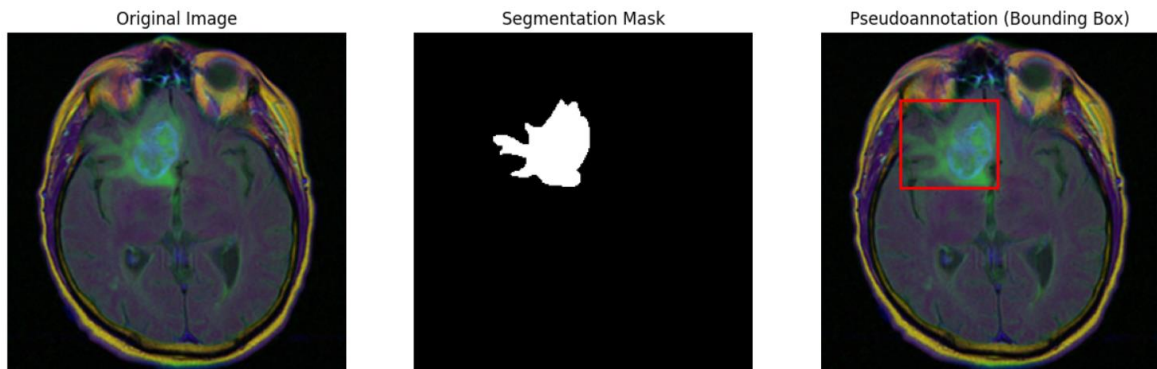

Figure 4.2.1. Pseudoannotaion using segmentaiton mask

The model was then trained according to Code 4.1.1., with the change of using the `lgg_dataset.yaml` file. Details related to the graphics card and hyperparameters remain the same as in Chapter 4.1.

The obtained `best.pt` model was used to run inference on test data of the LGG Segmentation Dataset. The provided bounding boxes were further used as input to the prompt encoder of the MedSAM model. The examples, as well as a comparison to the first model, will be given in Chapter 4.3.

4.3. Model comparison

To determine the region of interest, it is necessary to send a bounding box to the prompt encoder of the MedSAM model. To do that, two RCS-YOLO models were trained, and their comparison will be given in the following text. The first model was trained on the BR35H dataset (Model 1), and the second was trained based on pseudoannotation obtained from LGG Segmentation Dataset masks (Model 2). Both approaches are explained in the Chapters 4.1. and 4.2. The inference was run on the LGG Segmentation Dataset test set as mentioned in Chapter 4.2. The test set consists of 275 examples. Firstly, examples will be shown and then the comparison of the two detection models will be proposed.

In the figures 4.3.1. and 4.3.2. are given examples of the pseudoannotated bounding box, predicted bounding boxes (Model 1: blue, Model 2: red), ground truth mask, and predicted masks using the combination of models and MedSAM.

Model 2 appears to provide better bounding boxes than Model 1. Also, Model 1 often misses the target area or provides a larger or smaller bounding box compared to the pseudoannotation. This will be discussed further when comparing the models using the metrics listed below.
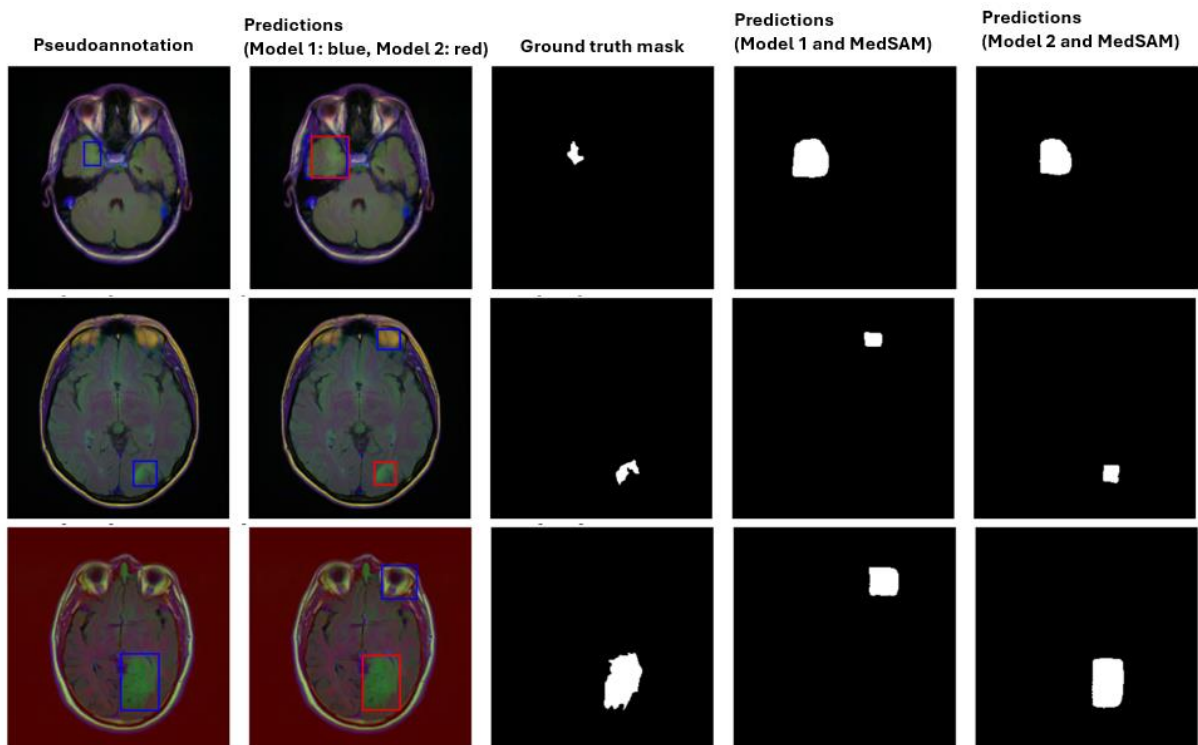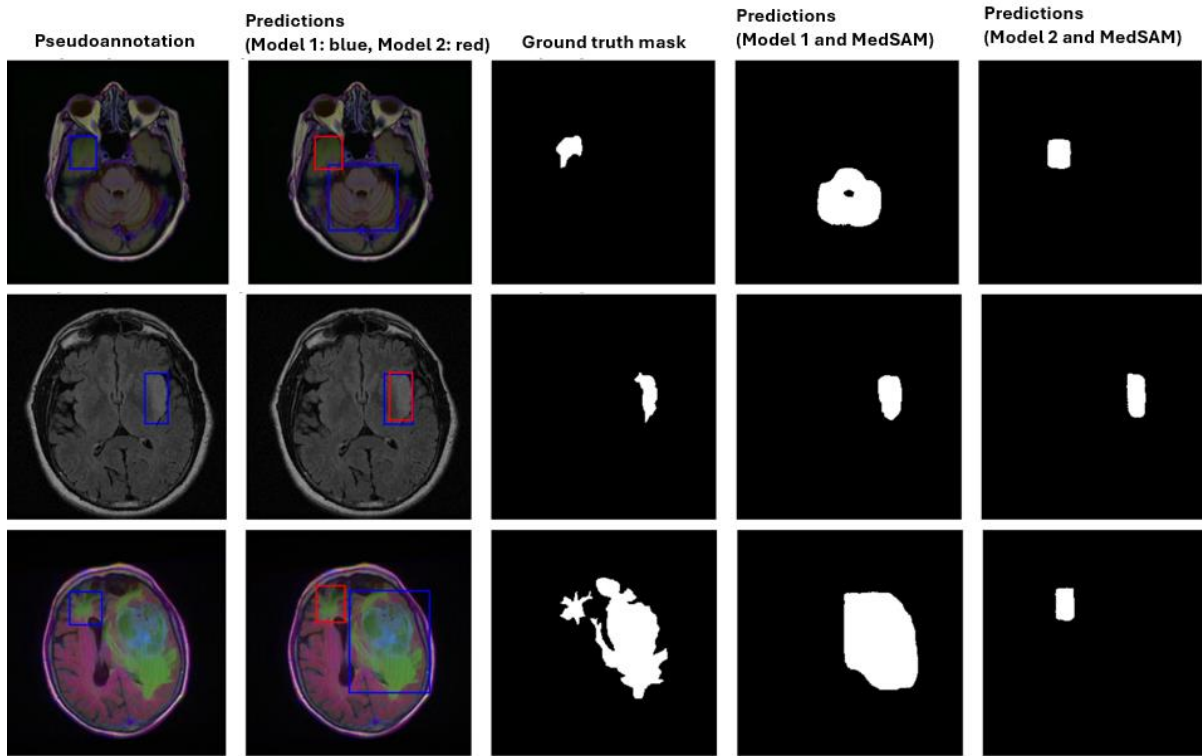

Figure 4.3.1. Examples of predictions

Figure 4.3.2. Examples of predictions

In this Chapter, the focus will not be on the quality of segmentation masks, but on finding sufficiently accurate detector that can be used in the process of automating the extraction of suspicious brain regions. For this purpose, the following metrics [81] are used:

$$P = \frac{TP}{TP + FP} = \frac{TP}{all\ detections}$$

(1)

$$R = \frac{TP}{TP + FN} = \frac{TP}{all\ ground\ truths}$$

(2)

$$mAP = \frac{1}{N} \sum_{i=1}^{N} AP_i$$

(3)

Precision (1) is the ability of the model to identify only relevant objects, and it is represented as a percentage of correct positive predictions. [81]

Recall (2) is the ability of the model to find all relevant cases, i.e. ground truth bounding boxes, and it is represented by the percentage of correct positive predictions among all given ground truths. [81]

The mean AP (mAP) (3) is represented as the average AP over all classes and represents the metric used to measure the accuracy of object detectors over all classes. [81] The mAP50 measures model accuracy considering only the "easy" detections, i.e. one with an intersection over union (IoU) threshold of 0.50. The mAP50-95 gives the model performance across different levels of detection difficulty. [82]

In the Table 4.3.1. the performances of Model 1 and Model 2 are given. Model 2 outperforms Model 1 in all the metrics, meaning that Model 2 has higher precision, recall, and accuracy (measured as mAP) at both 0.5 and 0.5:.95 thresholds.

Metrics / Models	P (Precision)	R (Recall)	mAP@.5	mAP@.5:.95
Model 1	0.819	0.182	0.168	0.101
Model 2	0.905	0.869	0.86	0.622

Table 4.3.1. Model 1 and Model 2 performances

Considering the results (Table 4.3.1.) and examples (Figures 4.3.1. and 4.3.2.) Model 2 combined with MedSAM appears to provide better results that are closer to the ground truth. The shapes and locations of predicted masks are more accurate than the ones obtained from the combination of Model 1 and MedSAM. Because of the mentioned, the combination of Model 2 and MedSAM will be used in further work.

5. Practical implementation

Practical implementation refers to the creation of a functional demo application for faster analysis of potentially suspicious MRI images. The provided GUI was developed using a PyQt5 framework. In the following subchapters, the PyQt5 framework and the functionalities of the application will be explained in more detail. It should be noted that the presented demo application only shows how the process of reviewing MRI images can be accelerated, but the presence of an expert is necessary for its practical application.

5.1. PyQt5

Qt represents a set of cross-platform C++ libraries that implement various high-level APIs, such as location and positioning services, multimedia, NFC and Bluetooth connectivity, a Chromium based web browser, and traditional UI development. PyQt5 is a set of Python bindings for Qt v5, and it consists of more than 35 extension modules which enables Python to be used as a development language for iOS and Android. [83] PyQt5 was used in the process of making a demo application, and some of the used features of PyQt5 are:

- QtWidgets: provides UI elements to create user interface with the use of Widgets – primary elements for creating user interfaces in Qt. [84] QtWidgets has many functions, and there are many subclasses such as QLabel, QPushButton, QWidget, etc.
- QtGui: offers classes for integration with the window system and event handling. It also supports OpenGL and OpenGL ES, 2D graphics, as well as basic imaging, fonts, and text. [85]
- QtCore: a system for object communication known as signals and slots. It provides object properties that can be queried and designed. Additionally, it includes a dynamic casting mechanism that functions across different library boundaries. [86]

5.2. Demo application

The main idea of the thesis was to try to automate the MRI examination process to determine abnormalities, i.e. brain tumors. For this purpose, the RCS-YOLO model was trained using pseudoannotations obtained from the LGG Segmentation Dataset. A pretrained MedSAM model was used for image segmentation. The reason for choosing a combination of these two models is explained in Chapter 4. Furthermore, the application was made using PyQt5 as mentioned in Chapter 5.1. Two images from the test data that was mentioned in Chapter 4.2. were used to create the demo application. Also, a conversion from .tif to .png format was made.

It should be noted that the `MedSAM_inference.py` script has been modified, so now it processes entire batches of images with YOLO format annotations (`x_center`, `y_center`, `width`, `height`).

The demo application is a tool designed to assist in the annotation and segmentation of suspicious MRI images. It contains image folder loading functionality, which makes multiple image processing easier. The "Image:" part of the application displays the image name of the image that contains a suspicious area. Furthermore, there is a three-column layout for displaying the original, detected, and segmented images. There are also navigation buttons implemented, so the "Previous Image" and "Next Image" buttons allow users to navigate through suspicious images in the loaded folder. Also, there are "Save annotation" and "Segment" buttons that will be explained later in the chapter. The user interface is shown in Figure 5.2.1.
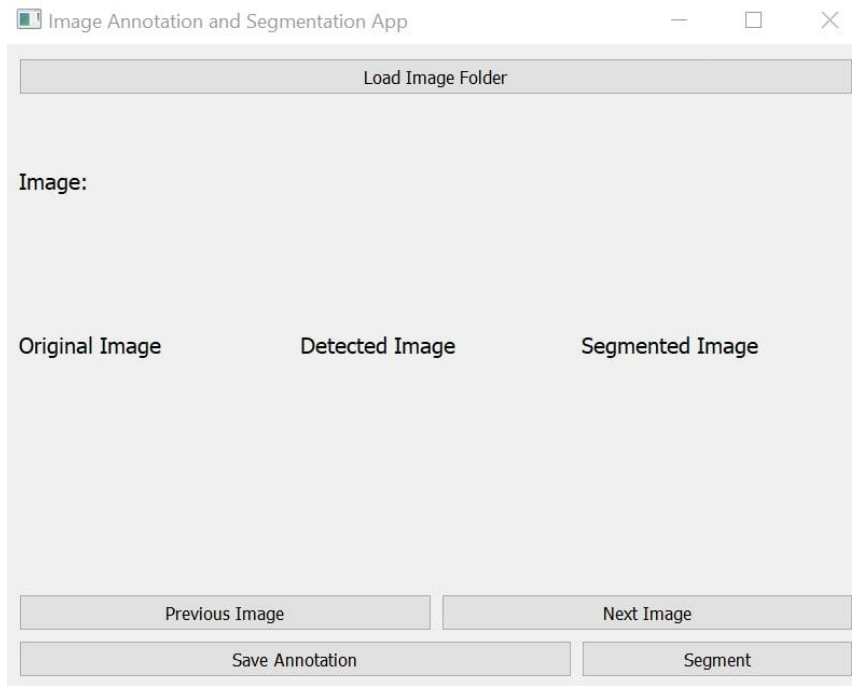
Figure 5.2.1. User interface - demo application

As earlier said, the idea of the demo application is to load a folder of images for which RCS-YOLO then tries to determine the suspicious area if it exists. Those suspicious images are then displayed in the application, as can be seen in Figure 5.2.2. In the "Original Image" column the image is shown as received, without any modifications, and in the "Detected Image" column the image is shown including the suspicious region marked with a bounding box.
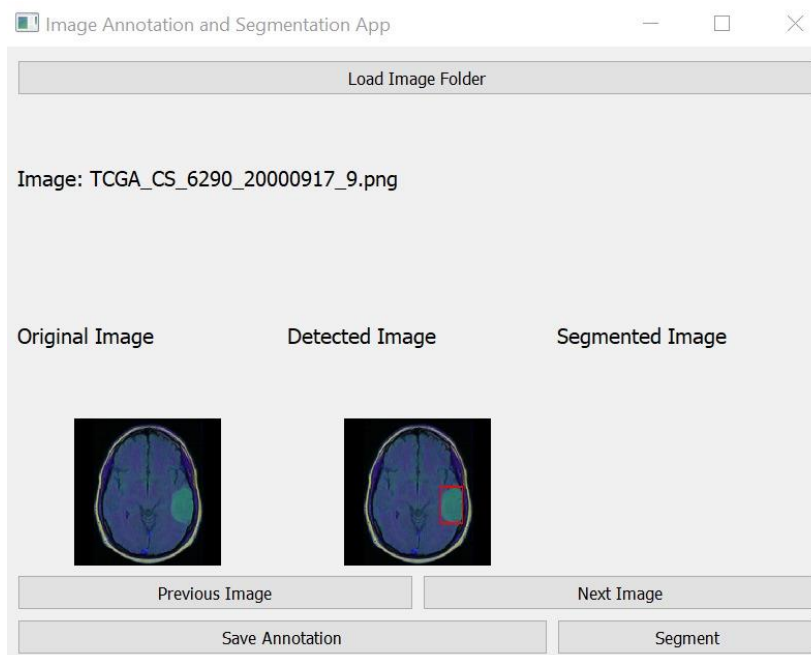

Figure 5.2.2. Display of the original and detected suspicious images

Furthermore, on the obtained images is possible to segment the marked suspicious area. The "Segment" button that was mentioned earlier triggers the segmentation process for the currently displayed image using the MedSAM model. After the segmentation process, the Detailed view is shown (Figure 5.2.3.). The "Segmented Image" column then shows the image after segmentation, highlighting the specific area that was previously marked as suspicious (Figure 5.2.4.).
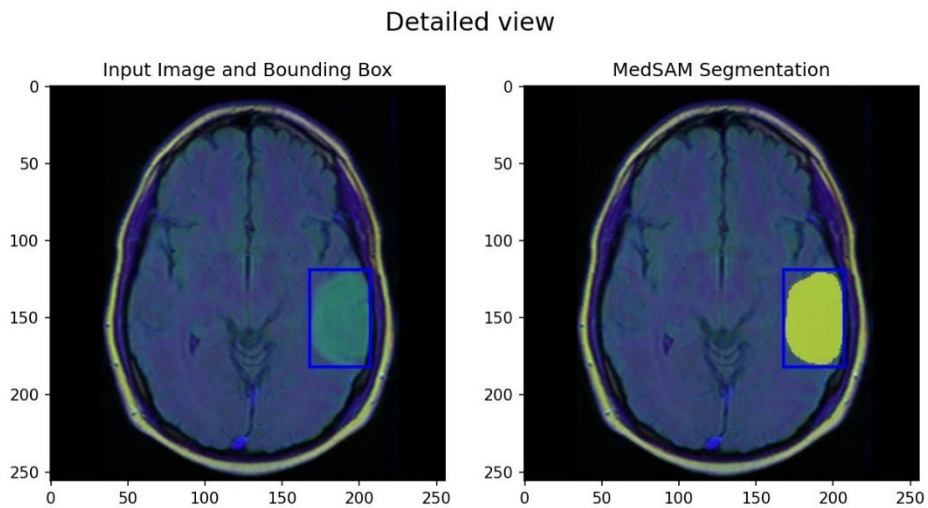

Figure 5.2.3. Detailed view of segmented area

Figure 5.2.4. Display of the original, detected and segmented suspicious images

Moreover, it is important to mention the "Save Annotation" possibility that allows users to save annotations they make. The saved image is shown in Figure 5.2.5.
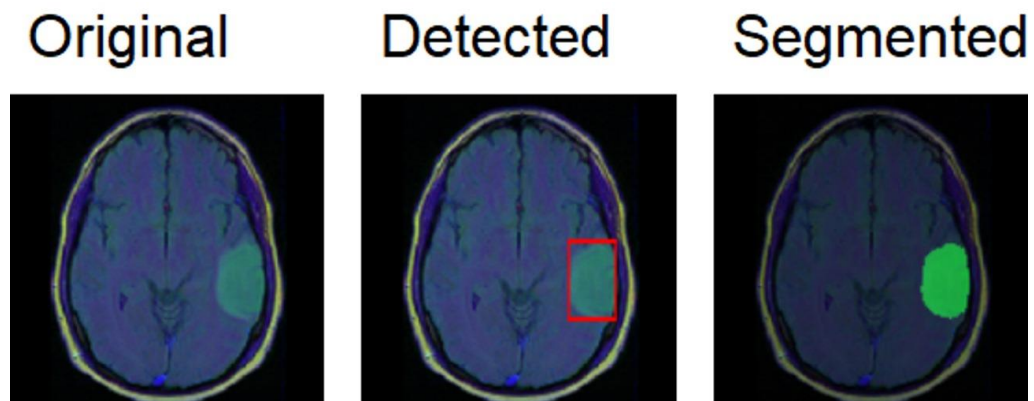

Figure 5.2.5. Display of the saved image

Consider that the demo version of the application requires more work to reach its full potential and fully meet the challenges of speeding up the process of annotating suspicious MRI images at a satisfactory level. Also, it should be noted that in addition to the implemented functionalities, the possibility of manually annotating the region of interest should also be implemented, which would be part of future work.

Overall, the demo version of the application provides the basis for successful acceleration of the annotation process of the large datasets of MRI images, which can also be a great help to the experts in the field. Also, it is important to note that the application can serve as an auxiliary tool, but a detailed examination of suspicious and non-suspicious images by an expert is mandatory.

6. Limitations

The thesis provides an idea of a comprehensive approach to speeding up the process of annotating suspicious MRI images. However, it's important to recognize the limitations of the thesis as well. Some of the main limitations are related to the dataset, the detection and segmentation model, the absence of experts, etc. Further details will be provided below.

To begin with, the problem of a dataset will be addressed. It cannot be stated that the LGG Segmentation Dataset was excluded from the training of the MedSAM model. Therefore, there is a possibility that the test set used here may have been part of the training process for the MedSAM model. Additionally, a significant limitation is the problem of finding a suitable annotated dataset, especially one obtained by an expert who also ensured data anonymization. Also, concern is the quality of the images in the dataset, as they may contain noise created by the imaging device.

The next limitation is related to the quality of the models used. Firstly, the obtained detections, i.e. regions of interest are not of satisfactory quality. The examples are given in the Figure 6.1. Insufficient quality of the pseudoannotations obtained from the LGG dataset segmentation masks could have contributed to this problem. This refers to Model 2 which was trained using these pseudoannotations and was later used in the demo application. Secondly, no comparison is provided between the obtained segmentation masks and the ground truth. Also, in the Figure 6.1. can be seen that the segmentation directly depends on the detected region of interest, and it doesn't follow the shape of the ground truth suspicious area. Note that often segmentation mask follows the shape of the detected area. Perhaps adding padding to the bounding box would give more context for MedSAM to distinguish the suspicious region from the rest of the brain.

Further limitations refer to ethical problems and problems related to the speed of obtaining annotations. Regarding ethical issues, the previously mentioned data anonymization represents a problem. Also, it should be noted that the annotations that were obtained need to be validated by experts. Another major issue is the possibility of bias and the insufficient precision of the used models.
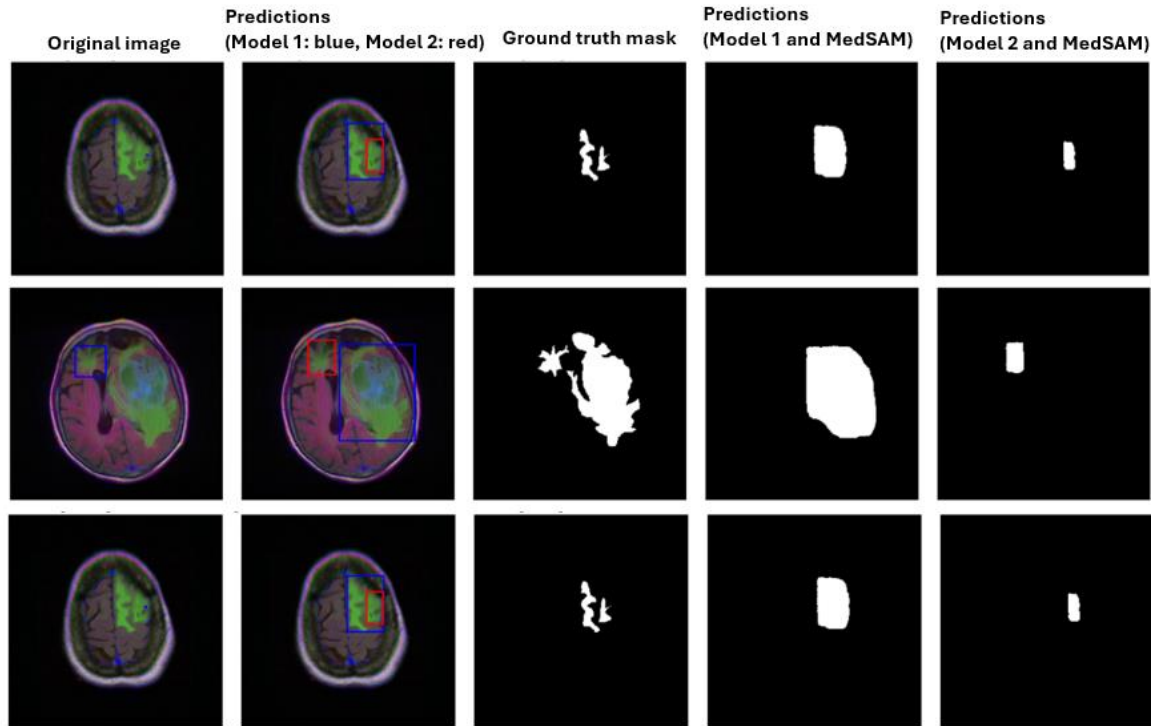
Figure 6.1. Examples of the obtained bounding boxes and segmentation masks

Lastly, the annotation speed is not validated, which can be a major limitation considering that the main idea is to speed up the process of annotating suspicious MRI images.

Some of the mentioned limitations will be addressed in Chapter 7, where potential solutions will be presented.

7. Future work

The thesis provides insights into the possibility of speeding up the annotation process of suspicious MRI images with the help of state-of-the-art models.

The primary direction of future work involves including experts in the development process of a comprehensive application, aimed at speeding up the process of extracting and analyzing suspicious MRI images.

Further work could expand the possibilities of the current demo application and make it a comprehensive annotation tool that would serve expert in the diagnostic process. To do that, it is necessary to implement additional capabilities such as manual marking of the region of interest for the following segmentation. Also, the possibility of annotating larger datasets should be implemented. Accordingly, it is necessary to monitor the time required for the annotation, particularly as the size of the dataset increases. It is important to implement the functionality of saving non-suspicious images, thus allowing further investigation if needed.

In Chapter 6 the limitations are discussed, and potential solutions are mentioned below.

Firstly, identifying or creating a high-quality, expert-validated annotated dataset is essential for effective model training. Also, denoising techniques can be used to improve image quality. Moreover, training the RCS-YOLO model on negative sample images could positively impact its performance. Regarding the MedSAM model performance, it is necessary to consider the quality of the obtained segmentation masks. One idea would be to add padding to the region of interest, i.e. bounding box, to contextually separate the suspicious area from the rest of the image.

The implementation of the mentioned, along with its application to other organs and tissues, could play a crucial role in efficient diagnosis. This can be crucial for the timely treatment of different types of diseases.

Conclusion

The thesis explores methods that aim to improve the efficiency and accuracy of segmenting suspicious regions in MRI brain tumor images by utilizing state-of-the-art models. The chosen segmentation model is MedSAM, which takes the detections obtained from RCS-YOLO model into a prompt encoder as a region of interest to perform further segmentation. The combination of those two models shows the potential to be used for the automatic analysis of the large MRI dataset to reduce data processing time while enhancing the precision of abnormality identification.

The integration of earlier-mentioned models into a demo application highlights the potential for further development of comprehensive tools. However, some limitations require further consideration. In particular, the models require additional evaluation to ensure the ability of handling a wide range of medical images and conditions effectively.

Future work aims to include experts in the development process of comprehensive applications. Also, the expansion of the current possibilities of the demo application is necessary, so the application can have the possibility of annotating larger datasets, as well as possibility of manually marking regions of interest for further investigation. Additionally, the capability to monitor the speed and performance of the process is essential for the improvement of the demo application. The focus will also be on improving the robustness of the algorithms and expanding their application to other types of medical images.

In conclusion, this thesis gives a starting point for the development of more sophisticated diagnostic tools that can improve both the speed and accuracy of medical image analysis, which can result in timely treatment and better patient care.

Literature

[1] Page, M.J., Mckenzie, J.E., Bossuyt, P.M., Boutron, I., Hoffmann, T.C., Mulrow, C.D., et al. *The PRISMA 2020 statement: an updated guideline for reporting systematic reviews*. BMJ, 372, n71. https://doi.org/10.1136/bmj.n71

[2] Verma, A., Shivhare, S.N., Singh, S.P., Kumar, N., Nayyar, A. *Comprehensive Review on MRI-Based Brain Tumor Segmentation: A Comparative Study from 2017 Onwards.* Archives of Computational Methods In Engineering. https://doi.org/10.1007/s11831-024-10128-0

[3] Gordillo, N., Montseny, E., Sobrevilla, P. (2013). *State of the art survey on MRI brain tumor segmentation*. Magn Reason Imaging 31(8):1426-1438. https://doi.org/10.1016/j.mri.2013.05.002

[4] Bonte, S., Van Holen, R., Goethals, I. (2018.) *Brain tumour segmentation on contrast enhanced T1w MRI using local texture and Random Forests*. ECR 2018, European congress of radiology. https://doi.org/10.1594/ecr2018/C-2343

[5] Usman, K., Rajpoot, K. (2017.) *Brain tumor classification from multi-modality MRI using wavelets and machine learning*. Pattern Analysis and Applications, 20(3), 871-881. https://doi.org/10.1007/s10044-017-0597-8

[6] Ma, C., Luo, G., Wang, K. (2018) *Concatenated and Connected Random Forests With Multiscale Patch Driven Active Contour Model for Automated Brain Tumor Segmentation of MR Images*. IEEE Transactions on Medical Imaging, vol. 37, no. 8, pp. 1943-1954, https://doi.org/10.1109/TMI.2018.2805821

[7] Soltaninejad, M., Yang, G., Lambrou, T., Allinson, N., Jones, T.L., Barrick, T.R., Howe, F.A., Ye, X. (2018) *Supervised learning based multimodal MRI brain tumour segmentation using texture features from supervoxels*. Comput Methods Programs Biomed. 2018 Apr;157:69-84. https://doi.org/10.1016/j.cmpb.2018.01.003

[8] Zhao, J., Meng, Z., Wei, L., Sun, C., Zou, Q., Su, R. (2019) *Supervised brain tumor segmentation based on gradient and context-sensitive features*. Frontiers in Neuroscience, 13, Article 144. https://doi.org/10.3389/fnins.2019.00144

[9] Samanta, A.K., Khan, A.A. (2018.) *Computer aided diagnostic system for automatic detection of brain tumor through MRI using clustering based segmentation technique and SVM classifier*. The International Conference on Advanced Machine Learning Technologies and Applications. https://doi.org/10.1007/978-3-319-74690-6_34

[10] Pandiselvi, T., Maheswaran, R. (2019.) *Efficient Framework for Identifying, Locating, Detecting and Classifying MRI Brain Tumor in MRI Images*. https://doi.org/10.1007/s10916-019-1253-1

[11] Rao, C.S., Karunakara, K. (2022.) *Efficient Detection and Classification on Brain Tumor using Kernel based SVM for MRI*. Multimedia Tools and Applications. https://doi.org/10.1007/s11042-021-11821-z

[12] Arunkumar, N., Mohammed, M.A., Mostafa, S.A., Ibrahim, D.A., Rodrigues, J.J., Albuquerque, V.H.C. (2020.) *Fully automatic model-based segmentation and classification approach for MRI brain tumor using artificial neural networks*.

Concurrency and Computation: Practice and Experience, 32(1), 4962. https://doi.org/10.1002/cpe.4962

[13] Mallick, P.K., Ryu, S.H., Satapathy, S.K., Mishra, S., Nguyen, G.N., Tiwari, P. (2019.) *Brain MRI Image Classification for Cancer Detection Using Deep Wavelet Autoencoder-Based Deep Neural Network*. IEEE, vol. 7, pp. 46278-46287, https://doi.org/10.1109/ACCESS.2019.2902252

[14] Santhosh Kumar, H.S., Karibasappa, K. (2022.) *An effective hybrid deep learning with adaptive search and rescue for brain tumor detection*. Multimedia Tools and Applications 81(13):17669-17701. https://doi.org/10.1007/s11042-022-12474-2

[15] Kumar, T.S., Arun, C., Ezhumalai, P. (2022.) *An approach for brain tumor detection using optimal feature selection and optimized deep belief network*. Biomedical Signal Processing and Control 73:103440. https://doi.org/10.1016/j.bspc.2021.103440

[16] Alagarsamy, S., Zhang, Y.-D., Govindaraj, V., Rajasekaran, M.P., Sankaran, S. (2020.) *Smart identification of topographically variant anomalies in brain magnetic resonance imaging using a fish school-based fuzzy clustering approach*. IEEE Transactions on Fuzzy Systems. https://doi.org/10.1109/TFUZZ.2020.3015591

[17] Hamad, Y.A., Simonov, K.V., Naeem, M.B. (2019.) *Detection of brain tumor in MRI images, using a combination of fuzzy c-means and thresholding*. International Journal of Advanced Pervasive and Ubiquitous Computing. https://doi.org/10.4018/IJAPUC.2019010104

[18] Sandhya, G., Kande, G.B., Satya, S.T. (2019.) *An efficient MRI brain tumor segmentation by the fusion of active contour model and self-organizing map*. Journal of Biomimetics, Biomaterials and Biomedical Engineering. https://doi.org/10.4028/www.scientific.net/JBBBE.40.79

[19] Faragallah, O.S., El-Hoseny, H.M., El-sayed, H.S. (2023.) *Efficient brain tumor segmentation using Otsu and K-means clustering in homomorphic transform*. Biomedical signal processing and control. https://doi.org/10.1016/j.bspc.2023.104712

[20] Tseng, C.J., Tang, C. (2023.) *An optimized XGBoost technique for accurate brain tumor detection using feature selection and image segmentation*. Healthcare Analytics. https://doi.org/10.1016/j.health.2023.100217

[21] Alex, V., Chennamsetty, S.S., Krishnamurthi, G. (2017.) *Generative adversial networks for brain lesion detection*. Medical Imaging. https://doi.org/10.1117/12.2254487

[22] Han, C., Rundo, L., Araki, R., Nagano, Y., Furukawa, Y., Mauri, G., Nakayama, H., Hayashi, H. (2019.) *Combining noise-to-image and image-to-image GANS: brain MR image augmentation for tumor detection*. https://doi.org/10.48550/arXiv.1905.13456

[23] Nema, S., Dudhane, A., Murala, S., Naidu, S. (2020.) *Rescuenet: an unpaired GAN for brain tumor segmentation*. Biomedical Signal Processing and Control. https://doi.org/10.1016/j.bspc.2019.101641

[24] Ding, Y., Zhang, C., Cao, M., Wang, Y., Chen, D., Zhang, N., Qin, Z. (2021.) *Tostagan: an end-to-end two-stage generative adversarial network for brain tumor segmentation*. Neurocomputing 462:141–153. https://doi.org/10.1016/j.neucom.2021.07.066

[25] Wu, X., Bi, L., Fulham, M., Feng, D.D., Zhou, L., Kim, J. (2021.) *Unsupervised brain tumor segmentation using a symmetric-driven adversarial network*. Neurocomputing 455:242–254. https://doi.org/10.1016/j.neucom.2021.05.073

[26] Chen, G., Ru, J., Zhou, Y., Rekik, I., Pan, Z., Liu, X., Lin, Y., Lu, B., Shi, J. (2021.) *Mtans: multi-scale mean teacher combined adversarial network with shape-aware embedding for semi-supervised brain lesion segmentation*. Neuroimage 244:118568. https://doi.org/10.1016/j.neuroimage.2021.118568

[27] Neelima, G., Chigurukota, D.R., Maram, B., Girirajan, B. (2022.) *Optimal deepmrseg based tumor segmentation with GAN for brain tumor classification*. Biomedical Signal Processing and Control 74:103537. https://doi.org/10.1016/j.bspc.2022.103537

[28] Wang, F., Huang, S., Shi, L., Fan, W. (2017.) *The application of series multi-pooling convolutional neural networks for medical image segmentation*. International Journal of Distributed Sensor Networks 13(12):1550147717748899 https://doi.org/10.1177/1550147717748899

[29] Zhao, X., Wu, Y., Song, G., Li, Z., Zhang, Y., Fan, Y. (2018.) *A deep learning model integrating FCNNS and CRFS for brain tumor segmentation*. Medical Image Analysis 43:98–111 https://doi.org/10.1016/j.media.2017.10.002

[30] Charron, O., Lallement, A., Jarnet, D., Noblet, V., Clavier, J.-B., Meyer, P. (2018.) *Automatic detection and segmentation of brain metastases on multimodal MR images with a deep convolutional neural network*. Computers in Biology and Medicine 95:43–54 https://doi.org/10.1016/j.compbiomed.2018.02.004

[31] Cui, S., Mao, L., Jiang, J., Liu, C., Xiong, S. (2018.) *Automatic semantic segmentation of brain gliomas from MRI images using a deep cascaded neural network*. Journal of Healthcare Engineering 2018:14 https://doi.org/10.1155/2018/4940593

[32] Hussain, S., Anwar, S.M., Majid, M. (2018.) *Segmentation of glioma tumors in brain using deep convolutional neural network*. Neurocomputing 282:248–261 https://doi.org/10.48550/arXiv.1708.00377

[33] Iqbal, S., Ghani, M.U., Saba, T., Rehman, A. (2018.) *Brain tumor segmentation in multi-spectral MRI using convolutional neural networks (CNN)*. Microscopy Research and Technique 81(4):419–427 https://doi.org/10.1002/jemt.22994

[34] Naceur, M.B., Saouli, R., Akil, M., Kachouri, R. (2018) *Fully automatic brain tumor segmentation using end-to-end incremental deep neural networks in MRI images*. Computer Methods and Programs in Biomedicine 166:39–49 https://doi.org/10.1016/j.cmpb.2018.09.007

[35] Kamnitsas, K., Ferrante, E., Parisot, S., Ledig, C., Nori, A.V., Criminisi, A., Rueckert, D., Glocker, B. (2016.) *Deepmedic for brain tumor segmentation.* In: Brainlesion: glioma, multiple sclerosis, stroke and traumatic brain injuries. https://doi.org/10.1007/978-3-319-55524-9_14

[36] Pereira, S., Oliveira, A., Alves, V., Silva, C.A. (2017.) *On hierarchical brain tumor segmentation in MRI using fully convolutional neural networks: a preliminary study*. In: 2017 IEEE 5th Portuguese meeting on bioengineering (ENBENG), IEEE. pp 1–4. https://doi.org/10.1109/ENBENG.2017.7889452

[37] Mittal, M., Goyal, L.M., Kaur, S., Kaur, I., Verma, A., Hemanth, D.J. (2019.) *Deep learning based enhanced tumor segmentation approach for MR brain images*. Applied Soft Computing 78:346–354. https://doi.org/10.1016/j.asoc.2019.02.036

[38] Togacar, M., Ergen, B., Comert, Z. (2020.) *BrainMRNet: brain tumor detection using magnetic resonance images with a novel convolutional neural network model*. Medical Hypotheses 134:109531. https://doi.org/10.1016/j.mehy.2019.109531

[39] Huang, Z., Liu, Y., Song, G., Zhao, Y. (2021.) *Gammanet: an intensity-invariance deep neural network for computer-aided brain tumor segmentation*. Optik 243:167441. https://doi.org/10.1016/j.ijleo.2021.167441

[40] Rafi, A., Madni, T.M., Janjua, U.I., Ali, M.J., Abid, M.N. (2021.) *Multi-level dilated convolutional neural network for brain tumour segmentation and multi-view-based radiomics for overall survival prediction*. International Journal of Imaging Systems and Technology 31(3):1519–1535. https://doi.org/10.1002/ima.22549

[41] Hu, K., Gan, Q., Zhang, Y., Deng, S., Xiao, F., Huang, W., Cao, C., Gao, X. (2019.) *Brain tumor segmentation using multi-cascaded convolutional neural networks and conditional random field*. IEEE Access 7:92615–92629. https://doi.org/10.1109/ACCESS.2019.2927433

[42] Ranjbarzadeh, R., Bagherian Kasgari, A., Jafarzadeh Ghoushchi, S., Anari, S., Naseri, M., Bendechache, M. (2021.) *Brain tumor segmentation based on deep learning and an attention mechanism using MRI multi-modalities brain images*. Scientific Reports 11(1):1–17. https://doi.org/10.1038/s41598-021-90428-8

[43] Deng, W., Shi, Q., Wang, M., Zheng, B., Ning, N. (2020.) *Deep learning-based HCNN and CRF-RRNN model for brain tumor segmentation*. IEEE Access 8:26665–26675. https://doi.org/10.1109/ACCESS.2020.2966879

[44] Khan, H., Shah, P.M., Shah, M.A., Islam, S., Rodrigues, J.J. (2020.) *Cascading handcrafted features and convolutional neural network for IoT-enabled brain tumor segmentation*. Computer Communications 153:196–207. https://doi.org/10.1016/j.comcom.2020.01.013

[45] Myronenko, A., Hatamizadeh, A. (2019.) *Robust semantic segmentation of brain tumor regions from 3d MRIs*. In: Brainlesion: glioma, multiple sclerosis, stroke and traumatic brain injuries. Springer. pp 82–89. https://doi.org/10.1007/978-3-030-46643-5_8

[46] Aswani, K., Menaka, D. (2021.) *A dual autoencoder and singular value decomposition based feature optimization for the segmentation of brain tumor from MRI images*. BMC Medical Imaging 21(1):1–11. https://doi.org/10.1186/s12880-021-00614-3

[47] Huang, D., Wang, M., Zhang, L., Li, H., Ye, M., Li, A. (2021.) *Learning rich features with hybrid loss for brain tumor segmentation*. BMC Medical Informatics and Decision Making 21(2):1–13. https://doi.org/10.1186/s12911-021-01431-y

[48] Aggarwal, M., Tiwari, A.K., Sarathi, M.P., Bijalwan, A. (2023.) *An early detection and segmentation of brain tumor using deep neural network*. BMC Medical Informatics and Decision Making 23(1):1–12. https://doi.org/10.1186/s12911-023-02174-8

[49] Lu, Y., Chang, Y., Zheng, Z., Sun, Y., Zhao, M., Yu, B., Tian, C., Zhang, Y. (2023.) *GMetaNet: multi-scale ghost convolutional neural network with auxiliary*

metaformer decoding path for brain tumor segmentation. Biomedical Signal Processing and Control 83:104694. https://doi.org/10.1016/j.bspc.2023.104694

[50] Boehringer, A.S., Sanaat, A., Arabi, H., Zaidi, H. (2023.) *An active learning approach to train a deep learning algorithm for tumor segmentation from brain MR images*. Insights Imaging 14(1):141. https://doi.org/10.1186/s13244-023-01487-6

[51] Bhandari, A., Koppen, J., Agzarian, M. (2020.) *Convolutional neural networks for brain tumour segmentation*. Insights Imaging **11**, 77. https://doi.org/10.1186/s13244-020-00869-4

[52] Ronneberger, O., Fischer, P., Brox, T. (2015.) *U-net: Convolutional networks for biomedical image segmentation*. In: International Conference on Medical Image Computing and Computer-assisted Intervention, pp 234–241. https://doi.org/10.48550/arXiv.1505.04597

[53] Zhu, W., Zhao, C., Li, W., Roth, H., Xu, Z., Xu, D. (2020.) *Lamp: Large deep nets with automated model parallelism for image segmentation*. In: International Conference on Medical Image Computing and Computer-Assisted Intervention, pp 374–384. https://doi.org/10.1007/978-3-030-59719-1_37

[54] Liu, P., Dou, Q., Wang, Q., Heng, P.-A. (2020.) *An encoder-decoder neural network with 3d squeeze-and-excitation and deep supervision for brain tumor segmentation*. IEEE Access 8:34029–34037. https://doi.org/10.1109/ACCESS.2020.2973707

[55] Naser, M.A., Deen, M.J. (2020.) *Brain tumor segmentation and grading of lower-grade glioma using deep learning in MRI images*. Computers in Biology and Medicine 121:103758. https://doi.org/10.1016/j.compbiomed.2020.103758

[56] Zhang, J., Jiang, Z., Dong, J., Hou, Y., Liu, B. (2020.) *Attention gate ResU-Net for automatic MRI brain tumor segmentation*. IEEE Access 8:58533–58545. https://doi.org/10.1109/ACCESS.2020.2983075

[57] Lin, C.-W., Hong, Y., Liu, J. (2021.) *Aggregation-and-attention network for brain tumor segmentation*. BMC Medical Imaging 21(1):1–12. https://doi.org/10.1186/s12880-021-00639-8

[58] Ma, S., Tang, J., Guo, F. (2021.) *Multi-task deep supervision on attention r2u-net for brain tumor segmentation*. Frontiers in Oncology 11:3651. https://doi.org/10.3389/fonc.2021.704850

[59] Rai, H.M., Chatterjee, K., Dashkevich, S. (2021.) *Automatic and accurate abnormality detection from brain MR images using a novel hybrid unetresnext-50 deep CNN model*. Biomedical Signal Processing and Control 66:102477. https://doi.org/10.1016/j.bspc.2021.102477

[60] Saeed, M.U., Ali, G., Bin, W., Almotiri, S.H., AlGhamdi, M.A., Nagra, A.A., Masood, K., Amin, Ru. (2021.) *RMU-NET: a novel residual mobile u-net model for brain tumor segmentation from MR images*. Electronics 10(16):1962. https://doi.org/10.3390/electronics10161962

[61] Xiao, Z., He, K., Liu, J., Zhang, W. (2021.) *Multi-view hierarchical split network for brain tumor segmentation*. Biomedical Signal Processing and Control 69:102897. https://doi.org/10.1016/j.bspc.2021.102897

[62] Zhou, T., Canu, S., Vera, P., Ruan, S. (2021.) *Feature-enhanced generation and multi-modality fusion based deep neural network for brain tumor segmentation with*

missing mr modalities. Neurocomputing 466:102–112. https://doi.org/10.1016/j.neucom.2021.09.032

[63] Aboelenein, N.M., Songhao, P., Afifi, A. (2022.) *IRDNU-Net: Inception residual dense nested u-net for brain tumor segmentation*. Multimedia Tools Appl pp 1–17. https://doi.org/10.1007/s11042-022-12586-9

[64] Aboelenein, N.M., Piao, S., Noor, A., Ahmed, P.N. (2022.) *MIRAU-Net: An improved neural network based on U-Net for gliomas segmentation*. Signal Processing 101:116553. https://doi.org/10.1016/j.image.2021.116553

[65] Cao, T., Wang, G., Ren, L., Li, Y., Wang, H. (2022.) *Brain tumor magnetic resonance image segmentation by a multiscale contextual attention module combined with a deep residual UNET (MCA-RESUNET)*. Physics in Medicine & Biology. https://doi.org/10.1088/1361-6560/ac5e5c

[66] Qin, C., Wu, Y., Liao, W., Zeng, J., Liang, S., Zhang, X. (2022.) *Improved U-Net3+ with stage residual for brain tumor segmentation*. BMC Medical Imaging 22(1):1–15. https://doi.org/10.1186/s12880-022-00738-0

[67] Wang, J., Yu, Z., Luan, Z., Ren, J., Zhao, Y., Yu, G. (2022.) *RDAU-Net: Based on a residual convolutional neural network with DFP and CBAM for brain tumor segmentation*. Front Oncol 210. https://doi.org/10.3389/fonc.2022.805263

[68] Ruba, T., Tamilselvi, R., Beham, M.P. (2023.) *Brain tumor segmentation using JGate-AttResUNet - A novel deep learning approach*. Biomedical Signal Processing Control 84:104926. https://doi.org/10.1016/j.bspc.2023.104926

[69] Yu, X., Yang, Q., Zhou, Y., Cai, L.Y., Gao, R., Lee, H.H., Li, T., Bao, S., Xu, Z., Lasko, T.A. et al (2023.) *UNesT: local spatial representation learning with hierarchical transformer for efficient medical segmentation*. Medical Image Analysis 90:102939. https://doi.org/10.48550/arXiv.2209.14378

[70] Ilhan, U., Ilhan, A. (2017.) *Brain tumor segmentation based on a new threshold approach*. Procedia Computer Science 120:580–587. https://doi.org/10.1016/j.procs.2017.11.282

[71] Nabizadeh, N., Kubat, M. (2017.) *Automatic tumor segmentation in single-spectral MRI using a texture-based and contour-based algorithm*. Expert Systems with Applications 77:1–10. https://doi.org/10.1016/j.eswa.2017.01.036

[72] Kistler, M., Bonaretti, S., Pfahrer, M., Niklaus, R., Büchler, P. (2013.) *The virtual skeleton database: an open access repository for biomedical research and collaboration*. Journal of Medical Internet Research 15(11):e245. https://doi.org/10.2196/jmir.2930

[73] B. H. Menze *et al.*, (2015.) *The Multimodal Brain Tumor Image Segmentation Benchmark (BRATS)*. *IEEE Transactions on Medical Imaging*, vol. 34, no. 10, pp. 1993-2024. https://doi.org/10.1109/TMI.2014.2377694

[74] Clark, K., Vendt, B., Smith, K., Freymann, J., Kirby, J., Koppel, P., Moore, S., Phillips, S., Maffitt, D., Pringle, M., Tarbox, L., Prior, F. (2013.) *The Cancer Imaging Archive (TCIA): maintaining and operating a public information repository*. Journal of Digital Imaging. 26(6):1045-57. https://doi.org/10.1007/s10278-013-9622-7

[75] Database, BWSB (2022.) https://brainweb.bic.mni.mcgill.ca . Accessed 21 Aug 2024

[76] Kang, M., Ting, C.-M., Ting, F. F., Phan, R.C.-W. (2023.) *RCS-YOLO: A Fast and High-Accuracy Object Detector for Brain Tumor Detection*. Medical Image Computing and Computer Assisted Intervention (pp. 664-674). https://doi.org/10.1007/978-3-031-43901-8_57

[77] Ma, J., He, Y., Li, F., Han, L., You, C., Wang, B. (2024.) *Segment Anything in Medical Images*. Nature Communications 15, 654. https://doi.org/10.1038/s41467-024-44824-z

[78] Hamanda, A. (2020.) Br53H: Brain Tumor Detection dataset. Kaggle. https://www.kaggle.com/datasets/ahmedhamada0/brain-tumor-detection . Accessed 26 Aug 2024

[79] Buda, M. (2019.) LGG Segmentation Dataset. Kaggle. https://www.kaggle.com/datasets/mateuszbuda/lgg-mri-segmentation . Accessed 26 Aug 2024

[80] Model Training with Ultralytics YOLO. Ultralytics. https://docs.ultralytics.com/modes/train/#augmentation-settings-and-hyperparameters . Accessed 27 Aug 2024

[81] Padilla, R., Netto, S. L., da Silva, E. A. B. (2020.) *A Survey on Performance Metrics for Object-Detection Algorithms*. International Conference on Systems, Signals and Image Processing (IWSSIP), Niteroi, Brazil, 2020, pp. 237-242, https://doi.org/10.1109/IWSSIP48289.2020.9145130

[82] YOLO Performance Metrics. Ultralytics. https://docs.ultralytics.com/guides/yolo-performance-metrics/#interpreting-the-output . Accessed 31 Aug 2024

[83] PyQt5, Version 5.15.7., Riverbank Computing. https://pypi.org/project/PyQt5/ . Accessed 1 Sept 2024

[84] QtWidgets, Qt Documentation. https://doc.qt.io/qt-6/qtwidgets-index.html . Accessed 1 Sept 2024

[85] Qt GUI Module. Qt Documentation. https://doc.qt.io/qt-5/qtgui-index.html . Accessed 1 Sept 2024

[86] Qt Core. Qt Documentation. https://doc.qt.io/qt-6/qtcore-index.html . Accessed 1 Sept 2024

[87] Database, BWSB (2022.). https://brainweb.bic.mni.mcgill.ca/cgi/brainweb1 Accessed 7 Sept 2024

[88] Cheng, J. (2017.). *Brain tumor dataset (version 5)*. https://figshare.com/articles/dataset/brain_tumor_dataset/1512427/5 Accessed 7 Sept 2024

[89] Chakrabarty, N. (2019.). *Brain MRI Images for Brain Tumor Detection*. https://www.kaggle.com/navoneel/brain-mri-images-for-brain-tumor-detection Accessed 7 Sept 2024

[90] Johanson, K.A., Becker, J.A. (2022.). *The whole brain atlas*. https://www.med.harvard.edu/aanlib/ Accessed 7 Sept 2024

[91] Simpson, A.L, Antonelli, M., Bakas, S., Bilello, M., Farahani, K., Van Ginneken, B., Kopp-Schneider, A., Landman, B.A., Litjens, G., Menze, B. et al (2019.). *A large annotated medical image dataset for the development and evaluation of segmentation algorithms*. https://doi.org/10.48550/arXiv.1902.09063

List of figures

List of tables